

Mathematical assessment of the impact of human-antibodies on sporogony during the within-mosquito dynamics of *Plasmodium falciparum* parasites

Miranda I. Teboh-Ewungkem¹, Woldegebriel A. Woldegerima^{2,3}, Gideon A. Ngwa⁴

¹ Department of Mathematics, Lehigh University, Bethlehem, PA, 18015, USA

² Department of Mathematics and Applied Mathematics, University of Pretoria, Hatfield 0028, Pretoria-South Africa *

³ Department of Mathematics, Mekelle University, P.o.box 231, Mekelle, Ethiopia

⁴ Department of Mathematics, University of Buea, P.O. Box 63, Buea, Cameroon

Abstract

We develop and analyze a deterministic ordinary differential equation mathematical model for the within-mosquito dynamics of the *Plasmodium falciparum* malaria parasite. Our model takes into account the action and effect of blood resident human-antibodies, ingested by the mosquito during a blood meal from humans, in inhibiting gamete fertilization. The model also captures subsequent developmental processes that lead to the different forms of the parasite within the mosquito. Continuous functions are used to model the switching transition from oocyst to sporozoites as well as human antibody density variations within the mosquito gut are proposed and used. In sum, our model integrates the developmental stages of the parasite within the mosquito such as gametogenesis, fertilization and sporogenesis culminating in the formation of sporozoites. Quantitative and qualitative analyses including a sensitivity analysis for influential parameters are performed. We quantify the average sporozoite load produced at the end of the within-mosquito malaria parasite's developmental stages. Our analysis shows that an increase in the efficiency of the ingested human antibodies in inhibiting fertilization within the mosquito's gut results in lowering the density of oocysts and hence sporozoites that are eventually produced by each mosquito vector. So, it is possible to control and limit oocysts development and hence sporozoites development within a mosquito by boosting the efficiency of antibodies as a pathway to the development of transmission-blocking vaccines which could potentially reduce oocysts prevalence among mosquitoes and hence reduce the transmission potential from mosquitoes to human.

Keywords: Malaria parasites, within-mosquito, sporogony, gametogenesis, human antibodies, transmission blocking, mathematical modelling

*Corresponding author: Cell phone: +27 (0) 627569977; e-mail: wa.woldegerima@up.ac.za

1 Introduction

The life cycle of *Plasmodium* parasites within a female *Anopheles* mosquito (the malaria vector) commences with the ingestion of mature (late stage) gametocytes by the mosquito during a blood meal from an infectious human. Once these malaria parasites are ingested by mosquito, they follow a prescribed developmental pathway leading to the formation of a new brood of the form the parasites, called sporozoites, in the mosquito that can be passed on to humans once the mosquito blood feeds on another human. The length of time required for the development of the parasite in the mosquito (the extrinsic incubation period) varies within and among *Plasmodium* species and is temperature dependent [8, 17].

The life cycle of *Plasmodium* commences with the ingestion of male and female *Plasmodium* gametocytes with a blood meal taken by a female *Anopheles* mosquito from an infectious human. Within the lumen of the mosquito's midgut, activation leading to gametogenesis occurs with each male gametocytes producing up to 8 micro (male) gametes and female gametocytes each producing 1 macro (female) gamete [8, 48]. About two hours after the blood meal, fertilization takes place with fusion between male and female gametes, producing zygotes [8, 10, 26]. The zygotes undergo meiosis and develop into the motile ookinetes, which further develop into oocysts. Oocysts then undergo multiple rounds of asexual replication resulting in the production of sporozoites - a process called *sporogony*. After completion of the sporozoite formation process, thousands of sporozoites are waiting in the oocyst to be released into the mosquito hemolymph [3, 43]. About $10^3 - 10^4$ sporozoites can be released per bursting oocyst [8, 9, 71, 73]. Sporozoites released in the mosquito hemocele then invade the salivary glands of the mosquito, where they mix with saliva ready to be injected into the next vertebrate host during a blood meal.

The life cycle within a human host commences when an infected female *Anopheles* mosquito injects sporozoites into the human's skin during feeding. Sporozoites enter the human's blood stream and are carried to the liver, where they infect liver cells, multiply within liver cells and the parasites develop into (hepatic) schizonts, which eventually rupture, releasing thousands of free merozoites into the human bloodstream [3, 8, 9, 26, 48, 65, 71]; on average 30,000 merozoites [30]. Released merozoites invade and infect the erythrocytes (RBCs) or die. The merozoites undergo asexual multiplication and develop into schizonts which eventually will rupture releasing 4 - 36 daughter merozoites [40], depending on the *Plasmodium* species, and invade fresh RBC to continue the asexual life cycle. Repeated cycles lead to depletion of healthy red blood cells thereby causing illness and potential death if not treated. During invasion of healthy erythrocytes by free merozoites, a proportion of merozoites inside the red blood cells switch to produce gametocyte stages - *the sexual stages infective to the mosquito vectors* [40].

In malaria regions, an infected human develops both cellular and humoral immune responses against pre-erythrocytic stages in the liver, erythrocytic and sexual stages parasites, with the immune responses that are acquired (adaptive) becoming increasingly well defined with repeated exposure to the parasite [5, 20, 25, 35, 39, 41, 42, 46, 66]. These acquired immunity can either inhibit parasitization of healthy liver cells by sporozoites, parasitization of healthy red blood cells by merozoites, reduction of parasitemia by elimination of merozoites and infected red blood cells or inhibition of the formation and/or maturation of gametocytes, [6, 15, 35, 41, 54, 82]. Its been reported that naturally acquired antibodies to the sexual stages of the malaria parasites within a human can interfere with the transmission of *Plasmodium* by female mosquitoes, where fertilization of gametes in the mosquitoes midgut can be blocked by cytokines and specific antibodies [5, 63]. That is, two major processes can mediate transmission-blocking immunity: (i) non-specific factors, such as cytokines that inhibit transmissibility of gametocytes to mosquitoes; and (ii) specific factors, which are naturally boosted by infection, whereby antibodies that can specifically recognize sexual stage parasite surface proteins block development of the parasite in the mosquito midgut [39]. Two broad categories

78 of parasite-derived molecules associated to transmission blocking immunity are identified in
79 [25]: immunity against proteins naturally boosted by infection expressed in gametocytes and
80 gametes; immunity against proteins expressed in mosquito-only parasite stages - gametes, zy-
81 gotes and ookinetes. The latter are never expressed in humans and thus free from human
82 immune pressures. Alternatively, when gametocytes that are not transmitted to mosquitoes
83 die, which is a vast majority of them, they release intracellular proteins/antigens into the host
84 circulation which could be boosted following immunization with a vaccine targeted to some
85 gametocyte antigens, providing long-lasting transmission-blocking immunity. These antigens
86 would then be processed and presented for recognition, eventually evoking humoral immune
87 responses which can be picked up together with mature gametocytes in a blood meal taken by
88 a feeding female mosquito [25, 41]. These acquired antibodies can substantially or completely
89 block gametogenesis and fertilization in the mosquito [8, 15, 13, 41, 47, 54] subsequently re-
90 ducing zygote production in the mosquito's midgut. If ingested gametocytes fail to start the
91 next phase of development within the mosquito's midgut, or fail to produce oocysts and hence
92 sporozoites, transmission is considered unsuccessful. This is the essence of transmission reduc-
93 ing immunity (TRI) and serves as a basis for the development of transmission blocking vaccines
94 (TBV) against parasite stages in the mosquito [20, 41]. In this manuscript, effective antibody
95 load/efficiency that would be considered as successful in inhibiting transmission would be a
96 load that would result in the production of less than one oocyst.

97 Factors such as the density of the gametocytes ingested as well as their viability, the presence
98 or lack of human antibodies in the ingested blood meal are all important factors play an
99 important role here [15, 29, 70, 71, 72, 73].

100 The search for vaccines against malaria parasites is ongoing and has been for decades with
101 different vaccines aimed at either the pre-erythrocytic stages, the blood stages or the mosquito
102 stages of the malaria parasite [7, 28, 31, 34, 44, 45, 55, 61, 58, 74, 79]. For example, there are
103 pre-erythrocytic vaccines aimed at inhibiting sporozoite infection, with the leading candidate
104 being the *RTS,S/AS01*, [7, 28, 45, 58, 74], which has demonstrated that it can reduce malaria
105 as well as severe life-threatening malaria in African children. Other pre-erythrocytic vaccines
106 target merozoite invasion, inhibiting the process via antibody activities, seeking to prevent the
107 progression of liver stage infections to blood stage infections. Yet again, others target infected
108 hepatocytes, killing them via T cell responses [27, 28]. Blood stage parasite vaccines aim to
109 prevent infected red blood cell (IRBC)-mediated pathology, conferring protection that would
110 reduce the severity of malaria episodes and/or parasitemia [27, 28].

111 There is hope of developing a vaccine that can either trigger an immune response that can de-
112 fend against the very first stages of parasitemia in humans, at the liver level (like the , or against
113 blood stage parasites or that interrupts malaria transmission from humans to mosquitoes, or
114 target the sexual sporogonic-mosquito (SSM) stages of the parasite in mosquitoes. Liver stage
115 vaccines, presumably act through T cell responses and possibly antibodies and prevent progres-
116 sion of liver stage infections to blood stage parasitemia, [27]. Vaccines against the mosquito
117 parasite stages aim at disrupting the within-mosquito parasite life cycle [18, 28, 27], with the
118 goal of reducing or eliminating the transmission potential of the parasites from mosquitoes to
119 humans. There vaccines are generally termed Transmission Blocking Vaccines (TBV). With
120 transmission blocking vaccines (TBV), the idea is that a vaccinated human will transfer induced
121 antibody-mediated immunity to a feeding mosquito during a successful blood meal and these
122 antibodies can serve to slow or block within-mosquito parasite development eventually slowing
123 or blocking transmission of the parasites (sporozoites) by the mosquito to another individual
124 [11, 16, 27, 38]. Various transmission blocking vaccine (TBV) candidates are currently under
125 investigation such as Pfs25, Pfs28, Pfs230, Pfs48/45, Pfs47, HAP2 and AnANP1 [1, 18, 28, 24].
126 Candidates Pfs230 and Pfs48/45 are antigens that begin their expression within a human host
127 in the intracellular gametocytes and induce antibody responses in humans that are naturally

128 exposed, meanwhile Pfs25 and Pfs28 are antigens that begin their expression in the mosquito
129 vector in the extracellular gametocytes. Among the aforementioned TBV candidates, Pfs230,
130 Pfs48/45 and Pfs25, are currently under development and aim to disrupt the fertilization pro-
131 cess, inhibiting zygote production [1]. The leading candidate is Pfs25, and it is in phase I
132 clinical trials, [18], where in early field clinical trials, a short-lived vaccine-induced antibody
133 functional response was demonstrated in mosquito-feeding assays. Current development fo-
134 cuses on improving the methods and vaccine delivery systems in order to generate long-lasting
135 immune responses [18, 27].

136 As for the candidate Pfs28, antibodies against it were not found to be effective although
137 they enhanced the transmission blocking activity of the antibodies against Pfs25. The TBV
138 candidates Pfs47, HAP2 and AnANP1 are recent discoveries and they are all expressed by
139 within-mosquito parasites: Pfs47 and HAP2 target zygote development while AnANP1 is a
140 mosquito midgut antigen [1].

141 Efficient control and management of malaria and related problems require that more eco-
142 nomical and reliable methods be used [50, 68]. Development of new control strategies would
143 entail a good understanding of the mechanisms that characterise malaria transmission and
144 the associated parameters. More realistic and robust mathematical models can play a role in
145 forecasting and designing of new strategies in Investigating the dynamics of the different de-
146 velopmental stages of the *Plasmodium falciparum* parasite within the mosquito. Even though
147 several articles exist on mathematical modelling of the population dynamics of the malaria
148 vector or the vector itself, (see, for example, [4, 49, 50, 51]), the literature on mathematical
149 models for the within mosquito-host dynamics of the malaria parasites is scanty. To the best of
150 our knowledge, the first such model is found in the paper by Teboh-Ewungkem et al. [71, 73],
151 in which the authors developed a model that simulates the within-mosquito dynamics of *Plas-*
152 *modium falciparum* in an *Anopheles* mosquito by taking blood meal as input and the final
153 sporozoite load as output. The model in [71, 73] was subsequently used in [70, 72] to under-
154 stand the dynamic relationship between gametocyte sex-ratios, male gametocyte fecundity and
155 size of ingested gametocytes. Another paper worth mentioning is that by Childs et al. [19]
156 wherein the authors extended the work of Teboh-Ewungkem et al. [71, 73] to a stochastic for-
157 mulation and used it to study how the diversity of the within-human parasite forms picked up
158 by a feeding mosquito relates to the subsequent diversity of the mosquito parasite forms that
159 exit the mosquito. None of the aforementioned works quantified the impact ingested human
160 antibodies can have on the development and size of the within-mosquito parasite forms, a task
161 we aim to achieve in this manuscript. In so doing, we extend the model in [71, 73] by incor-
162 porating the potential impact of ingested human antibodies on the within-mosquito parasite
163 developmental and transition processes. The model, a system of non-linear continuous-time
164 ordinary differential equations, is then used to quantify oocysts density and sporozoites load
165 that can be produced by an infected mosquito at the end of the sporogonic cycle under human
166 adaptive immunity effects. We note here that much is repeated from [71, 73] for the sake of
167 completeness. The model accounts for transmission blocking interventions in general, which
168 may be as a result of natural infection that can be boosted with natural immunity or vaccines.
169 In general, transmission-blocking interventions (TBIs) that directly target the parasite can be
170 broadly classified as transmission-blocking vaccines (TBVs), discussed earlier, or transmission-
171 blocking drugs (TBDs) [25, 76]. As reported in [76], TBDs can be classified as follows: (i)
172 **Drugs targeting the malaria parasite within the human-host**; This category includes:
173 (a) drugs killing asexual stages of the parasite effectively and rapidly within human so that their
174 progression to gametocytes may be stopped/reduced; (b) drugs reducing the commitment of
175 asexual parasites to gametocytes within the human cycle, named as, the commitment blocking
176 drugs; (c) drugs directly targeting immature and mature (stage $I - V$) gametocytes within the
177 human; (d) drugs providing chemo-prophylaxis by directly acting on sporozoites, hence halting

178 establishment of infection inside the human [64, 76]. (ii) **Drugs targeting the vector itself**,
 179 which includes a special class of drugs known as *endectocides* [64, 76] (e.g. ivermectin), adminis-
 180 tered to humans that can kill a mosquito that draws blood from a human with the administered
 181 drug. Both (i) and (ii) are not the focus of this manuscript and would not be elaborated upon
 182 further. See [64, 76] for further details. (iii) **Drugs targeting the parasite in the vector**.
 183 This category comprises of antimalarial drugs that target the developmental stages (ingested
 184 gametocytes in the midgut of vector, male and female gametes, zygote, ookinete, oocyst and
 185 the sporozoites) of the parasite within mosquito vector [64, 76] and fall within the scope of our
 186 work.

187 The rest of this paper is organized as follows. In Section 2, formulation of the mathematical
 188 model is presented. The basic mathematical results and their detailed proofs are illustrated in
 189 the Appendix. Numerical simulations and result are presented in section 3 including the an
 190 estimate of the sporozoite density. A discussion of the results is presented in section 4 and we
 191 conclude in section section 5 giving ideas for future direction.

192 2 The Mathematical Model

193 Guided by the biology, the *Plasmodium falciparum* within-mosquito parasite forms are catego-
 194 rized at any time $t \geq 0$, into compartments described by the variables: G_{IM} , respectively, G_{IF} ,
 195 representing the densities of the late stage male, respectively, female *Plasmodium falciparum*
 196 gametocytes picked by a female *Anopheles* mosquito from an infectious human after a success-
 197 ful blood meal; G_M , respectively, G_F , representing the densities of male, respectively, female
 198 gametes that arise via gametogenesis from the respective gametocytes of identical gender after
 199 the blood meal has settled within the mosquito midgut; Z , the density of zygotes formed as a
 200 result of fertilization between male and female gametes; T , the density of ookinetes produced
 201 from zygotes within the mosquito; O , the density of oocysts produced from ookinetes, and S ,
 202 the density of salivary glands sporozoites, produced mature oocysts burst. A summary of the
 203 definitions of the state variables and their quasi-dimension is shown on Table 1. Throughout,
 204 we adopt the following measurement notations: time is measured in *days*, volume in micro-litre,
 205 μL , density of late stage gametocytes are measured in number of gametocytes per unit volume,
 206 denoted by $gam/\mu L := G$, densities of the developmental stages of the parasite within the
 207 mosquito (gametes, zygotes, ookinetes, oocysts, sporozoites) are measured by number of para-
 208 sites per volume (density of parasites), denoted by $pa/\mu L := P$ and density of human adaptive
 209 immune effectors within mosquito's midgut taken with blood measured in number of cells per
 210 unit volume denoted by $cells/\mu L := I$. Throughout this study, densities refer to number per
 211 volume of blood. We now describe the derivation of the equations governing the time rate of
 212 change of each of the identified state variables. The assumptions used are governed by the
 213 within-mosquito biology and past work, see [3, 8, 71, 80]. A conceptual schematic illustrating
 214 the flow dynamics of the within-mosquito developmental stages of the *P. falciparum* parasites
 215 is shown in Figure 1.

- (i) **Equation for male and female gametocytes:** When a female *Anopheles* mosquito bites an infected human, she may pick up the late stage (mature) gametocytes with the blood meal. If the blood meal contains both male (G_{IM} and female gametocytes G_{IF}) the within-mosquito vector dynamics can begin, upon successful insertion into the mosquito's gut. We assume that a mosquito picks an initial density of G_{I0} late stage gametocytes in a blood meal, which then decays exponentially thereafter. Of the ingested gametocytes, we assume that a fraction \tilde{m} are male while the remaining fraction $1 - \tilde{m}$ are female, so that the initial value of late stage male gametocytes ingested is $G_{IM}(0) = \tilde{m}G_{I0}$ and that of female gametocytes is $G_{IF}(0) = (1 - \tilde{m})G_{I0}$, respectively, with $G_{IM}(0) + G_{IF}(0) = G_{I0}$.

Variables	Description	Quasi-dimension
G_{IM}, G_{IF}	Density of late stage male (G_{IM}) and female (G_{IF}) gametocytes picked by a feeding mosquito after a successful blood meal that still remain as gametocytes at time $t \geq 0$.	G.
G_M, G_F	Densities of male (G_M) and female (G_F) gametes at time $t > 0$.	P
Z	Density of zygotes at time $t > 0$.	P
T	Density of ookinete at time $t > 0$.	P
O	Density of oocysts at time $t > 0$.	P
S	Density of salivary glands sporozoites at time $t > 0$.	P
E_a	Density of human adaptive immune effectors within mosquito's midgut taken with during a blood meal.	I

Table 1: Description of state variables and their quasi-dimensions.

The differential equation quantifying the time rate of change of the densities of the male female gametocytes thereafter take the forms $\frac{dG_{IM}}{dt} = -c_1 G_{IM}$, $G_{IM}(0) = \tilde{m}G_{I0}$, and $\frac{dG_{IF}}{dt} = -d_1 G_{IF}$, $G_{IF}(0) = (1 - \tilde{m})G_{I0}$, respectively, where c_1 is the rate at which male gametocytes exflagellate to produce male gametes while d_1 is the rate at which female gametocytes transform (emerge) to produce female gametes, both via gametogenesis. So, at any time $t \geq 0$, the respective densities of the male and female gametocytes in the mid gut of the mosquito are given by

$$G_{IM}(t) = \tilde{m}G_{I0}e^{-c_1 t}, \quad G_{IF}(t) = (1 - \tilde{m})G_{I0}e^{-d_1 t} \quad \forall t \geq 0, \quad (1)$$

- (ii) **Equation for the human antibodies:** We assume that the mosquito picks a density \tilde{E}_{a0} of antibodies (part of the adaptive immune cells) with the blood meal, and once it is inside the mosquito's gut, it decreases as time increases at a rate $\tilde{\beta}$, where $\tilde{\beta}$ is the rate at which the blood meal is digested. Thus, we have that $\frac{dE_a}{dt} = -\tilde{\beta}E_a(t)$, with initial condition $E(0) = \tilde{E}_{a0}$, so that the density of antibodies (adaptive immune response) inside the mosquito's midgut is

$$E_a(t) = \tilde{E}_{a0}e^{-\tilde{\beta}t}, \quad \forall t \geq 0. \quad (2)$$

- 216 (iii) **Equation for the densities of male and female gametes:** Within minutes of in-
217 gestion, the ingested gametocytes in a blood meal undergo **gametogenesis** [3, 8]. The
218 process starts and culminates with the female gametocytes producing ν_1 female gametes
219 (G_F) per female gametocytes within a 5 minutes after the blood meal, meanwhile the
220 male gametocytes exflagellate producing $s_1 \geq \nu_1 \geq 1$ male gametes (G_M) per gametocyte
221 about 10 minutes later [8]. Thus, male gametes emerge some 15 minutes after the blood
222 meal. Hence, during the period of gametogenesis, the density of late stage male and fe-
223 male gametocytes decrease (see [8]) and we assume the rates are c_1 and d_1 , respectively. It
224 is worth noting that compared to the female gamete produced, most of the male gametes
225 produced are not viable [8, 71, 73]. Let $\tilde{\alpha}_1$ be the fraction of the male gametes that are
226 viable and $\tilde{\alpha}_2$ be the fraction of the female gametes that are viable, then the effective
227 density of male gametes produced per male gametocytes is $s_1 c_1 \tilde{\alpha}_1$ while $\nu_1 d_1 \tilde{\alpha}_2$ is the ef-
228 fective density of female gametes produced per female gametocytes. Generated male and
229 female gametes can die at rates a_1 and b_1 , respectively, or before death, undergo the pro-
230 cess of fertilization. During fertilization, male and female gametes fuse to form a zygote

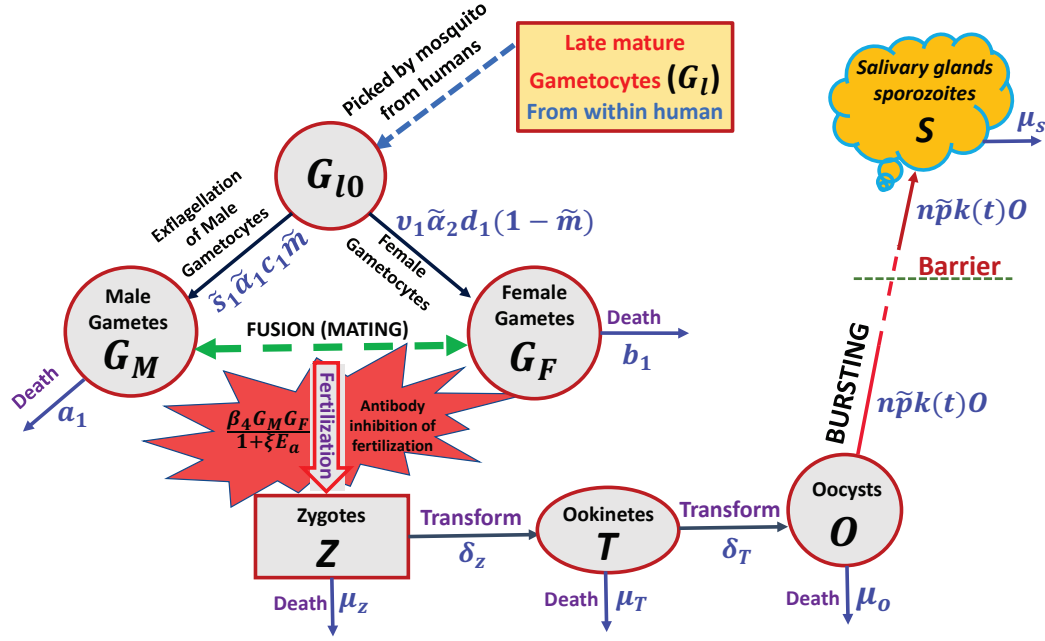


Figure 1: Flow diagram for the within mosquito developmental stages of malaria parasites. A proportion of the late stage matured gametocytes (male and female) picked by *Anopheles* mosquito used as an input for the starting point of the within mosquito cycle. Male gametocytes exflagellate via gametogenesis producing male gametes. A fusion of male and female gametes which leads to a generation of zygotes. Zygotes transform to motile ookinetes. Ookinetes establish oocysts, and then mitosis begins. The sporoblast forms and sporozoites will be produced. Sporozoites travel to the salivary gland and are available for transfer to humans during the next blood meal. The descriptions of the parameters are given in Table 2.

231 through gene mixing. According to the biological literature [8], fertilization and fusion
 232 occur in a approximately 75 minutes after the blood meal (i.e. within 60 minutes after
 233 male gametes emerge and 70 after female gametes emerge) and we denote the fertilization
 234 rate by β_4 . However, the process of fertilization can be inhibited by the human adaptive
 235 immune effectors picked up with the blood meal. We model this inhibition process by the
 236 factor $\frac{1}{1+\xi E_a}$, where ξ represents the efficiency of the inhibition process [8, 15, 47]. We
 237 note here that an effective antibody load/efficiency is considered to be when it results to
 238 the production of less than one oocyst.

Thus, the equations describing the densities of male (G_M) and female (G_F) gametes are, respectively, defined as:

$$\frac{dG_M}{dt} = s_1 \tilde{\alpha}_1 c_1 G_{IM} - a_1 G_M - \frac{\beta_4 G_M G_F}{1 + \xi E_a(t)}, \quad G_M(0) = 0 \quad (3)$$

and

$$\frac{dG_F}{dt} = \nu_1 \tilde{\alpha}_2 d_1 G_{IF} - b_1 G_F - \frac{\beta_4 G_M G_F}{1 + \xi E_a(t)}, \quad G_F(0) = 0. \quad (4)$$

239 (iv) **Equation for the density of zygotes:** The end product of a successful fertilization is
 240 the fusion of male and female gametes to form a zygote.

Zygotes can transform into motile ookinetes through the process of meiosis at rate δ_z , a process that takes between 10 – 30 hours [8, 71], or they can die naturally at a per capita rate μ_z . So, the equation governing the zygote population is

$$\frac{dZ}{dt} = \frac{\beta_4 G_M G_F}{1 + \xi E_a(t)} - \mu_z Z - \delta_z Z, \quad Z(0) = 0. \quad (5)$$

(v) **Equation for the density of ookinetes:** Mature ookinetes appear in approximately 20 hours after a blood meal [8, 75]. Those that successfully cross the peritrophic matrix after their migration through the blood meal enter the midgut epithelium where their transformation to oocysts commences. We denote the transformation rate of from ookinetes to oocysts by δ_T , and this process occurs approximately 24 – 48 hours after the blood meal. The unsuccessful ookinetes die at a per capita death rate of μ_T . Hence, the equation for the density of the ookinete stage parasites is:

$$\frac{dT}{dt} = \delta_z Z - \mu_T T - \delta_T T, \quad T(0) = 0. \quad (6)$$

(vi) **Equation for the density of oocysts:** Oocysts undergo extensive growth through mitosis and sporoblast formation, completes its development within 10 – 14 days [3] after the original blood meal, resulting in the production of thousands of sporozoites at a time dependent rate of $k(t)$. It is worth noting that other authors have reported 5 – 7 days [8] and 6 – 9 days [9]. Oocysts also die naturally at a per capita death rate of μ_o . It has been reported in [8, 9] that oocysts can survive the entire sporogony period. Thus, we the oocyst parasite population is modelled by

$$\frac{dO}{dt} = \delta_T T - \mu_o O - k(t)O, \quad O(0) = 0. \quad (7)$$

241 (vii) **Equation for the density of sporozoite:** Sporozoites will be released from oocysts
 242 within 1 – 2 weeks after a blood meal. Of these sporozoites produced per oocysts, only
 243 a fraction \tilde{p} of them make it to the salivary glands. Sporozoites die naturally at a rate
 244 μ_s . Once the sporozoites have reached the mosquito's salivary glands, they can survive
 245 there for the remainder of the life of the mosquito [8, 9] unless they are injected by the
 246 mosquito to a vertebrate host during the next bite by the mosquito for a blood meal.

247 The transformation rate of oocysts to produce sporozoites is represented here by a function
 248 $k(t)$ for all $t \geq 0$. To determine the nature of $k(t)$, we must examine more closely the
 249 events that lead to the formation of the sporozoites from the mature oocysts many days
 250 after the initial ingestion of the infected blood meal by an *Anopheles* mosquito [3, 8, 9].
 251 There is some variance in the timing as noted earlier: a range of 5 – 7 days was reported
 252 by [8], 6 – 9 days by [9] and 10 – 14 days by [3]. Since the end of sporoblast formation is
 253 the precursor to the realization of sporozoites formation, we shall use roughly the midway
 254 point in these times to assume that sporozoites can become available in the salivary glands
 255 of the mosquito at about the 10th day (a choice used in [71, 73]). We believe this is more
 256 reasonable also given how long a mosquito lives in the wild. Thus we shall assume that,
 257 once an oocyst matures and sporoblast formation commences, there is a very fast change
 258 around the 10th day of development to produce sporozoites. So, we can estimate a range
 259 for the rate of conversion from mature oocyst to produce sporozoites, $k(t)$, as:

$$k(t) = \begin{cases} 0, & \text{if } 0 \leq t < 10 - \varepsilon^2, \\ \frac{\kappa}{2\varepsilon^2}(t - 10 + \varepsilon^2), & \text{if } 10 - \varepsilon^2 \leq t < 10 + \varepsilon^2, \\ \kappa, & \text{if } t \geq 10 + \varepsilon^2 \end{cases} \quad (8)$$

with $\kappa \in [\frac{1}{9}, \frac{1}{7}]$ (see [71, 73]) and $0 < \varepsilon \ll 1$ is very small positive number showing that there is a rapid shift from almost no sporozoites to some amount of sporozoites at around $t = 10$ days. Hence, we write

$$\frac{dS}{dt} = n\tilde{p}k(t)O - \mu_s S, \quad S(0) = 0, \quad (9)$$

260 n is the number of sporozoites produced per bursting oocysts.

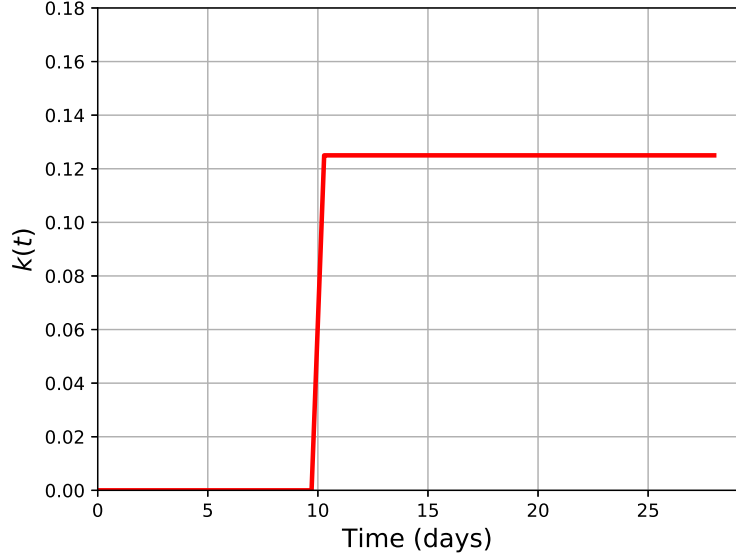


Figure 2: Plot of the time -dependent production rate function of sporozoites from mature oocysts, plotted for $\varepsilon = 1 \times 10^{-5}$, $\kappa = \frac{1}{8}$ as t runs from 0 to 28 days.

261 Therefore, all in one, the equations governing the developmental stage dynamics of malaria
 262 parasites within the mosquito is given by the non-linear system of ODEs:

$$\left. \begin{aligned}
 \frac{dG_{IM}}{dt} &= -c_1 G_{IM}, & G_{IM}(0) &= \tilde{m} G_{I0}, \\
 \frac{dG_{IF}}{dt} &= -d_1 G_{IF}, & G_{IF}(0) &= (1 - \tilde{m}) G_{I0}, \\
 \frac{dG_M}{dt} &= s_1 \tilde{\alpha}_1 c_1 G_{IM} - a_1 G_M - \frac{\beta_4 G_M G_F}{1 + \xi E_a(t)}, & G_M(0) &= 0, \\
 \frac{dG_F}{dt} &= \nu_1 \tilde{\alpha}_2 d_1 G_{IF} - b_1 G_F - \frac{\beta_4 G_M G_F}{1 + \xi E_a(t)}, & G_F(0) &= 0, \\
 \frac{dZ}{dt} &= \frac{\beta_4 G_M G_F}{1 + \xi E_a(t)} - \mu_z Z - \delta_z Z, & Z(0) &= 0, \\
 \frac{dT}{dt} &= \delta_z Z - \mu_T T - \delta_T T, & T(0) &= 0, \\
 \frac{dO}{dt} &= \delta_T T - \mu_O O - k(t) O, & O(0) &= 0, \\
 \frac{dS}{dt} &= n \tilde{p} k(t) O - \mu_s S, & S(0) &= 0, \\
 \frac{dE_a}{dt} &= -\tilde{\beta} E_a(t), & E(0) &= \tilde{E}_{a0},
 \end{aligned} \right\} \quad (10)$$

263 where, $E_a(t)$, the density of a human's adaptive immune response effectors within the mosquito's
 264 midgut at time t picked during a blood meal, is defined in equation (2). A summary of the
 265 parameters used in the model together with their descriptions and quasi-dimension is given in
 266 Table 2.

267 We note that the basic mathematical properties of system (10); positivity, boundedness and
 268 uniqueness of solutions, that ascertain that model solutions are mathematically and physically
 269 realizable are given in the Appendix. An analytic general solution, at least in integral form,
 270 also Appears in the Appendix.

Parameter	Description	Quasi-dimension
\tilde{E}_{a0}	Initial density of adaptive immune cells picked during blood meal.	I
G_{l0}	Initial density of gametocytes picked during blood meal.	G
$\tilde{\beta}$	Rate of decay of blood meal within mosquito gut.	$Time^{-1}$
\tilde{m}	Proportion of male gametocytes picked by the mosquito.	1
$1 - \tilde{m}$	Proportion of female gametocytes picked by the mosquito.	1
c_1	Rate at which male gametocytes transform (exflagellate) to produce male gametes via gametogenesis.	$Time^{-1}$
d_1	Rate at which female gametocytes transform (emerge) to produce female gametes via gametogenesis.	$Time^{-1}$
s_1	Number of male gametes produced per male gametocytes	$P \times G^{-1}$
ν_1	Number of female gametes produced per female gametocytes	$P \times G^{-1}$
$\tilde{\alpha}_1$	Fraction of male gametes that are viable	1
$\tilde{\alpha}_2$	Fraction of female gametes that are viable	1
a_1	Death rate/failure rate of male gametes	$Time^{-1}$
b_1	Death rate/failure rate of female gametes	$Time^{-1}$
β_4	Fertilization rate of male and female gametes	$P^{-1} \times Time^{-1}$
ξ	Efficiency of adaptive immune effectors in inhibiting fertilization	I^{-1}
μ_z	Zygote death rate	$Time^{-1}$
δ_z	Zygote transformation rate to ookinetes	$Time^{-1}$
δ_T	Ookinetes transformation rate to oocysts	$Time^{-1}$
μ_T	Ookinetes death rate	$Time^{-1}$
μ_o	Mature Oocysts death rate	$Time^{-1}$
$k(t)$	Mature Oocysts bursting rate	$Time^{-1}$
n	Number of sporozoites produced per bursting oocysts	1
\tilde{p}	Fraction of sporozoites that make it to the salivary glands	1
μ_s	Natural death rate of sporozoites	$Time^{-1}$

Table 2: Description of parameters and their quasi- dimensional units. We measure time in *days*, and volume in μL .

3 Numerical simulations, results and sensitivity analysis

The solutions to system (10) are obtained via numerical integration using the parameter values given in Table 3 and initial conditions given in Table 4. The feasible parameters obtained, guided by the biological literature, were discussed in detail in [71, 73]. Additionally, two parameters of interests appearing in model (10) are estimated and their sensitivity discussed. These two parameter are $E_a(0)$, the size of ingested human antibodies within a blood meal, and ξ , a parameter that measures the efficiency of the ingested antibody's functionality. One would expect these parameters to vary depending on the mechanism by which the human antibodies were generated; whether naturally initiated as a result of the human being naturally exposed to the malaria parasite [14, 57], or whether it was drug or vaccine initiated [12]. Moreover, it would also depend on the state of the human from whom the blood meal was taken, whether recently exposed or not [57]. The literature on the specific mentioned parameters are not copious. However, using information from [62], we will allow the number of ingested human antibodies to vary from a small size to 100 in a blood meal and the efficiency ξ to vary from zero to unity, in order to quantify their individual and combined impacts on the size of the number of oocysts produced in an infected mosquito. In what follows, we consider the dynamics

287 to be based on only a single blood meal taken by the feeding female anopheles mosquito. We
 288 understand that during their lifetime, mosquitoes feed on average every two to three days (see
 289 [53, 52, 67]), but we do not consider that here, except what happens when a single blood meal
 290 is taken. This is reasonable and informative and the results based on a single blood meal are
 291 easily extendable, when appropriate, to multiple blood meal feeding episodes if we consider the
 292 time lag between meals and the length of time it takes for mature oocysts to burst to release
 293 sporozoites (it takes about 10 days). That means oocysts that result from a second and hence
 294 subsequent blood meals would lag by about 2-3 days period for each additional blood meal, in
 295 their sporozoite production. One can then account for the total sporozoite load from two or
 296 more blood meals by summing up the sporozoites from the first, second and subsequent blood
 297 meals. Again, this assumption does not account for those mosquitoes that do not succeed in
 298 getting a full blood meal and live to seek again within a short time.

299 **3.1 The role of human antibodies in inhibiting fertilization of ga-** 300 **metes and sporozoite load**

301 **No antibody influence on within-mosquito fertilization and sporozoite load**

302 We begin this section with the numerical simulations when no antibody effects inhibit fertiliza-
 303 tion of male and female gametes within a mosquito, i.e. the term $\xi E_a(0) = 0$. Now, $\xi E_a(0) = 0$
 304 if either (i) $E_a(0) = 0$, that is no antibodies are ingested initially with the blood meal, or (ii)
 305 $\xi = 0$, that is the ingested antibodies' functionality in inhibiting fertilization and impacting
 306 parasite development within the mosquito is negligible. Another possibility is that both ξ and
 307 $E_a(0)$ are small so that their combined effect is negligible. The case $E_a(0) = 0$ can be thought
 308 of as a scenario in which a blood meal was taken by a female anopheles mosquito from an
 309 infected individual who was not recently exposed since per the results in [57] it was suggested
 310 that naturally acquired immunity against two of the antigens that begin their expression in
 311 intracellular gametocyte within naturally exposed human hosts, Pfs48/45 and Pfs230, was a
 312 function of recent exposure rather than of cumulative exposure to gametocytes. In the same
 313 article no age dependency This can manifest itself in areas of very low malaria transmission
 314 (hypoendemic regions) whereby due to the low transmission, the inhabitants are less exposed
 315 to infective mosquito bites when compared to a high transmission area where the inhabitants
 316 are more prone to infective mosquito bites. Thus, inhabitants in higher transmission regions
 317 have a higher propensity to have recent infections, even though the infections may not be severe
 318 for adults and children with a better defined adaptive immune response (see [33, 46, 66, 69] for
 319 more on naive and mature immune individuals and disease severity). On the other hand, the
 320 case $\xi = 0$ can represent a scenario in which the ingested antibodies are not at full functional
 321 performance level and this could be corrected with boosting of the naturally acquired sexual
 322 stage specific antibody response with boosting either via a TBD or TBV. In the absence of
 323 experimental measurements, a combined effect in which the product $\xi E_a(0) = 0$ might be more
 324 meaningful. Solution curves for the scenario in which $\xi E_a(0) = 0$ are shown in Figure 3. This
 325 basically reproduces figure 3 of [71].

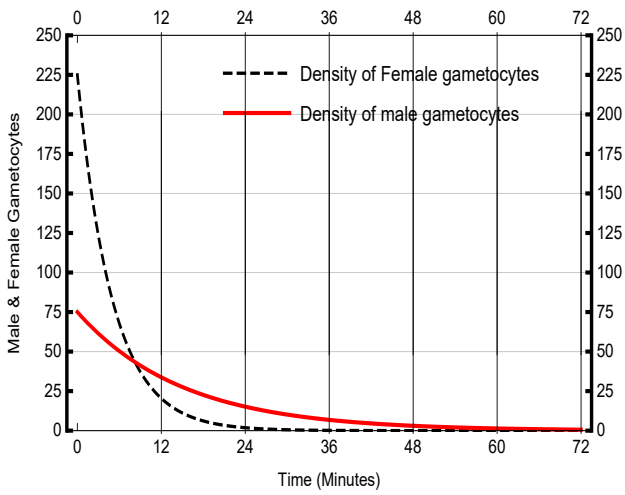
326 Subfigure 3a shows solution curves of the densities of late stage gametocytes in the mosquito
 327 midgut after a blood meal, plotted for 0.05 days, that is, approximately 72 minutes, a time frame
 328 that captures roughly the life span of gametocytes. The trajectories show that the densities
 329 of both male and female gametocytes decaying to zero within the plotted time. Subfigure 3b
 330 shows trajectories of densities of male and female gametes plotted in 0.08 days (about 1.9 hrs)
 331 which shows the female and male gamete population sizes increasing from zero to some bounds
 332 (as gametogenesis occurs) reaching their peaks slightly beyond 5 and 15 minutes, respectively,
 333 and then reducing back to zero. By the end of the last process, fertilization between male

Parameter	Range of values	Baseline value	Quasi-dimension	ref.
$\tilde{\beta}$	$[\frac{2}{3}, \frac{10}{2}]$	$\frac{10}{3}$	day^{-1}	estimated
\tilde{E}_{a0}	varies	11	$Cells/\mu L$	estimated
G_{l0}	[10, 1000]	300	$gam/\mu L$	[71]
\tilde{m}	(0, 0.5]	0.25	1	[70, 71]
$1 - \tilde{m}$	(0.5, 1]	0.75	1	[70, 71]
c_1	≈ 96	96	day^{-1}	[71]
d_1	≈ 288	288	day^{-1}	[71]
s_1	[4, 8]	8	$(para/\mu L) \times (gam/\mu L)^{-1}$	[71]
ν_1	1	1	$(para/\mu L) \times (gam/\mu L)^{-1}$	[71]
$\tilde{\alpha}_1$	(0, 4)	0.39	1	[71]
$\tilde{\alpha}_2$	(0, 1]	1	1	[71]
a_1	$[\frac{1440}{25}, \frac{1440}{15}]$	$\frac{1440}{20}$	day^{-1}	[71]
b_1	$[\frac{1440}{30}, \frac{1440}{20}]$	$\frac{1440}{25}$	day^{-1}	[71]
β_4	(0, 0.15]	0.08	$(para/\mu L)^{-1} \times day^{-1}$	[71]
ξ	[0, 1]	0, 0.8	$(Cells/\mu L)^{-1}$	[2]
μ_z	1	1	day^{-1}	[71]
δ_z	$[\frac{24}{23}, \frac{24}{19}]$	$\frac{24}{19}$	day^{-1}	[71]
μ_T	[1, 1.5]	1.4	day^{-1}	[71]
δ_T	[0.5, 1]	0.6	day^{-1}	[71]
μ_o	0	0	day^{-1}	[71]
$k(t)$	See eqn. (8)	See eqn. (8)	day^{-1}	[71]
κ	$[\frac{1}{9}, \frac{1}{7}]$	$\frac{1}{8}$	day^{-1}	[71]
ε^2	$[10^{-12}, 10^{-4}]$	10^{-5}	day	estimated
n	[1000, 10000]	3000	1	[71]
\tilde{p}	[0.1, 0.25]	0.2	1	[71]
μ_s	$[\frac{1}{6}, \frac{1}{4}]$	$\frac{1}{6}$	day^{-1}	estimated

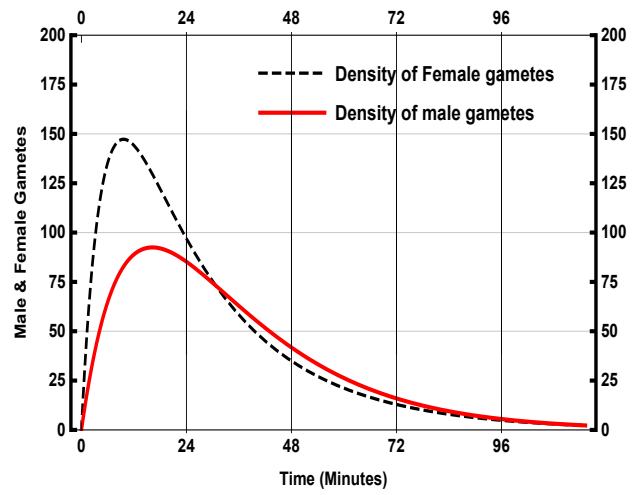
Table 3: Within mosquito host dynamics: Range and baseline of parameter values and their quasi- dimensional units. In [71], a detailed and elaborate description of the parameter ranges as well as the biological basis leading to the derivation of the ranges was presented. Thus, we do not repeat that here.

State variable	E_a	G_{lM}	G_{lF}	G_M	G_F	Z	T	O	S
Initial Value	\tilde{E}_{a0}	$\tilde{m}G_{l0}$	$(1 - \tilde{m})G_{l0}$	0	0	0	0	0	0

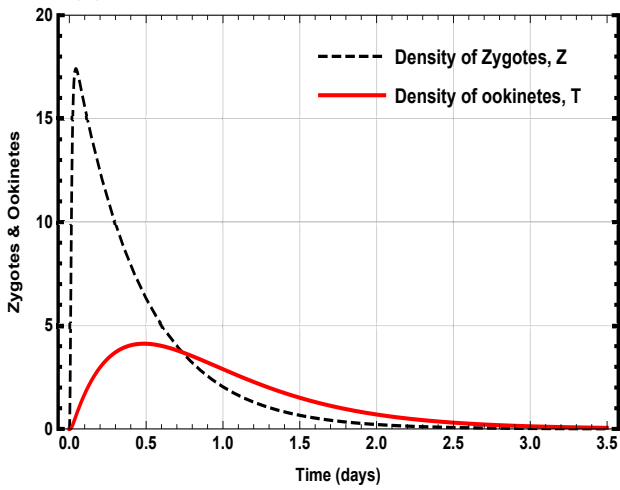
Table 4: Initial Conditions at time $t = 0$ for model (10) [71].



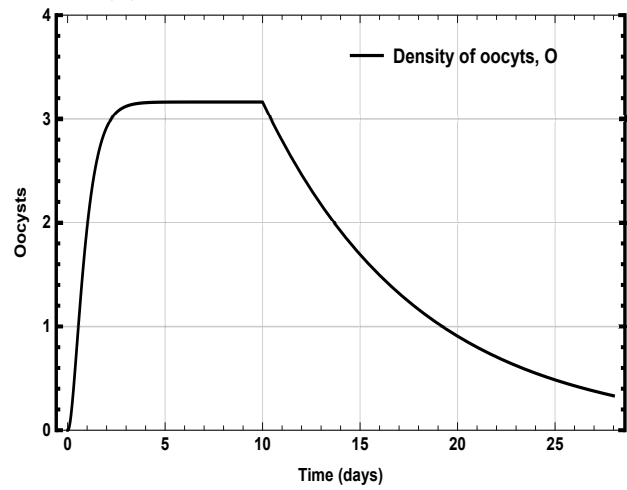
(a) Plot of male and female gametocytes



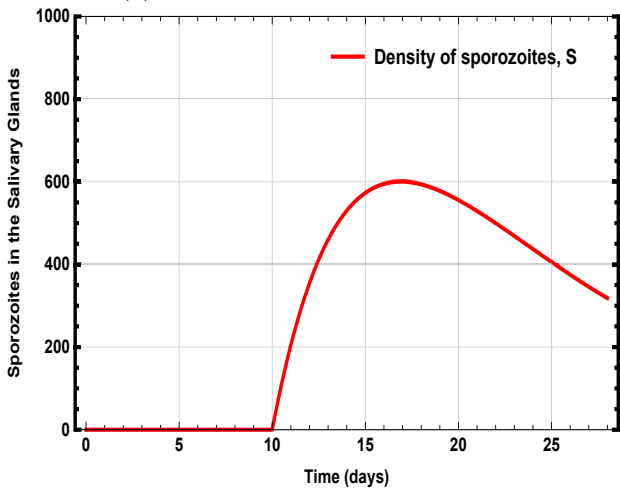
(b) Plot of male and female gametes



(c) Plot of zygotes and ookinetes



(d) Plot of oocysts



(e) Plot of sporozoites

Figure 3: Trajectory solutions of model system (10) in the case when $\xi = 0$ so that human antibodies/adaptive immune effectors have no effect on fertilization and zygote development of malaria parasites within the mosquito.

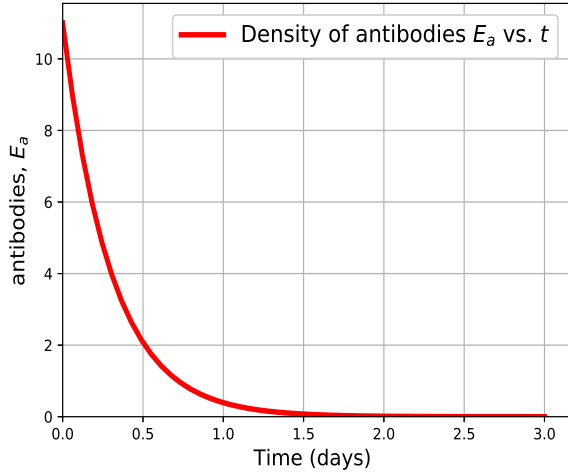
334 and female gametes occur producing zygotes. Zygotes density increases from zero to reach an
335 upper bound. The produced zygotes undergo meiosis to form ookinetes, the later, the progeny
336 of oocysts. Both zygotes and ookinetes drop to an average of less than by 1 each by day 2.
337 Their solution profiles are plotted in subfigure 3c. Subfigures 3d and 3e show trajectories for the
338 densities of oocysts and sporozoites, respectively plotted for a time period of 28 days which is
339 taken to represent the lifespan of a feeding female mosquito. Oocysts reach a maximum density
340 in approximately 2 days after a blood meal, a time within which mature oocysts are considered
341 to have been established and made entrance into the midgut epithelium [8, 71]. Mitosis begins
342 with sporoblast formation happening, and at about the 10th day, sporozoites are released from
343 bursting oocysts (see subfigures 3d and 3e). Sporozoites stay in the salivary glands until the
344 next mosquito bite or the mosquito dies.

345 **Antibody influence on within-mosquito fertilization and sporozoite load**

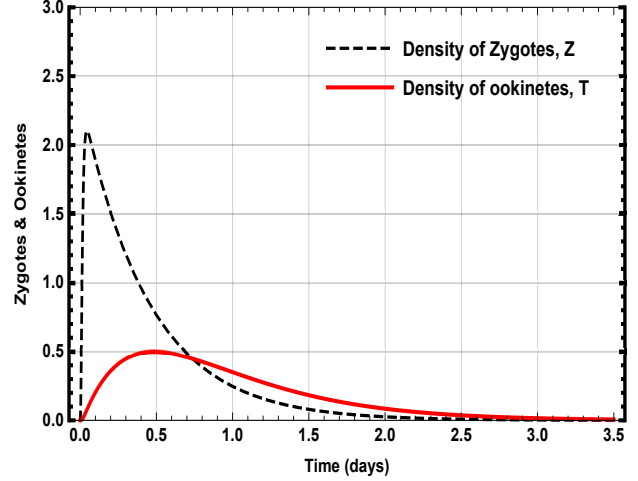
346 In this subsection, we consider the role of ingested antibodies and their potential impact on
347 fertilization of male and female gametes, and hence, subsequent within parasite development.
348 The profile for the ingested immune effectors are exponentially decaying functions, decaying
349 from $E_a(0) = 11$ (taken as the initial condition and baseline value) immune cells in an ingested
350 blood, as shown in Figure 4a, where blood meal sizes range from 2 to 10 μL [59, 71]. When
351 these antibodies/adaptive immune response play a role we consider the dimensionless term
352 $\xi E_a(0) = 8.8 \neq 0$, where $\xi = 0.8$ can be thought of as the efficiency with which the ingested
353 immune factors function and $E_a(0) = 11$ is the ingested number of antibodies. See Figures
354 4b - 4d for the solution curves for the zygote, ookinete and oocyst populations, as well as
355 the resulting sporozoite load, when antibody effects are considered. The choice of $\xi = 0.8$
356 was based on an electron microscopical study in [2] and also a study in [60]. We remark that
357 the studies were on *Plasmodium gallinaceum* and not *Plasmodium falciparum*, the parasite
358 under study in this manuscript. However, it gives us a starting point, especially with limited
359 information. Comparing Figure 3 to Figure 4, it is easy to see that the densities of zygotes,
360 ookinetes, oocysts and the sporozoite load all reduce significantly in the presence of antibodies.
361 Specifically, the maximum average zygote density of about 17.5 in the absence of antibodies
362 (subfigure 3c), reduces to approximately and average of 2.1 (subfigure 4b) when the effects of
363 antibodies are considered. Likewise, the ookinete peak reduces from about 4 (see subfigure
364 3c) with no antibody effect to approximately 0.5 (subfigure 4b) with antibodies assumed to
365 function at 80% efficiency, an 87.5% drop. Similar effects can be seen in the oocyst densities
366 (comparing subfigures 3d and 4c), with maximum peak of slightly above 5 reducing to under 1,
367 which in turn would yield fewer sporozoite load. The corresponding sporozoite peak densities
368 are approximately 600 (subfigure 3e) with no antibody effect, dropping to approximately 70
369 (subfigure 4d) with antibody effects. These drops in the sporozoite load do not only occur at
370 the peaks and endpoints, they occur at each time frame from the 10th day until the mosquito
371 dies. These illustrated decreases in the peak densities of the within-mosquito parasite forms
372 correlate with decreases in total population sizes of these forms. We note that compared to
373 the model in [71], the sporozoite peak density when no antibody effect is considered is slightly
374 lower in this manuscript (see subfigure 3e) compared to the corresponding sporozoite maximum
375 density in Fig. 3d of [71], which was at 1500 mainly because of the death term considered in
376 this model. We next compute the cumulative sporozoite sum.

377 **Estimation of the cumulative sum of sporozoite density**

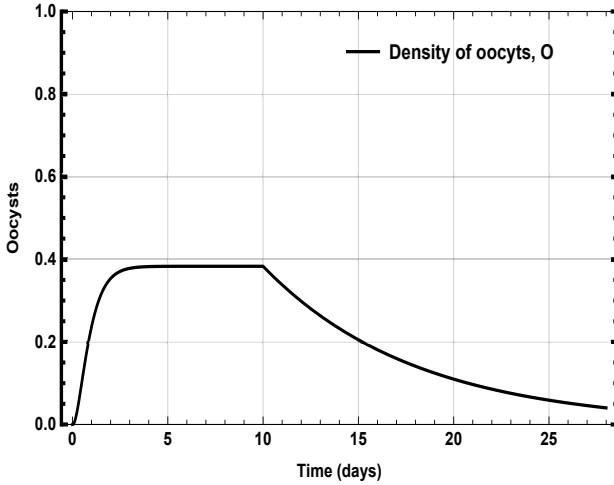
The end result of the within-mosquito processes after a blood meal from an infectious human is the production of sporozoites, the form of the parasite transmissible from mosquitoes to humans. Thus, it is desirable to estimate the cumulative sum of sporozoite density (or running



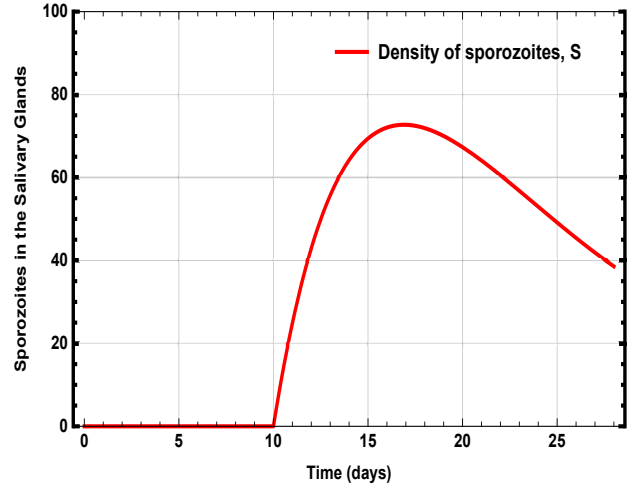
(a) Density of antibodies in the mosquito, $E_a(t)$ vs. time



(b) Plot of zygotes



(c) Plot of oocysts



(d) Plot of sporozoites

Figure 4: Solution curves of model system (10) in the case when $\xi = 80\%$.

total density), which we denote by S_{cumsum} . We will also compute the total, S_{area} , and average S_{avg} , sporozoite densities produced at the end of the within-mosquito process, based on a single blood meal. The effective average, which is the average over the time after oocysts release sporozoites would also be computed. We start with the computations of the total and average densities and compare the results for the case when no human antibody effects are in action, that is $\xi E_{a0} = 0$, and in when human antibody effects function to inhibit and slow fertilization. For the latter case, $\xi = 80\%$ and $E_{a0} = 11$ immune cells per ingested blood meal, so that $\xi E_{a0} = 8.8 \neq 0$. The estimate of the total sporozoite density produced, which is the area under the graph of the solution curves for $S(t)$ between the lines $t = 0$ and $t = t_{end} = 28$ days (see Subfigures 3e and 4d), and that of the average densities are computed via the respective functions,

$$S_{area} = S_{cumsum}(t_{end}) = \int_0^{t_{end}} S(t)dt \quad \text{and} \quad S_{avg} = \frac{1}{t_{end} - 0} \int_0^{t_{end}} S(t)dt.$$

378 These definite integrals are then estimated using the composite Simpson's rule in Python,
 379 were a step size of $h = 0.56$ was chosen, leading to the partitioning of the time interval $[0, 28]$

380 days into $n = 50$ sub intervals. For the case with no human effectors in effect, the cumulative
381 sum is $S_{area} = \int_0^{28} S(t)dt = 14,663.38$ sporozoites, yielding an average sporozoites density of
382 $S_{avg} = \frac{1}{28-0} \int_0^{28} S(t)dt = 523.69$ and an effective average density of $\frac{1}{28-10} \int_{10}^{28} S(t)dt = 814.63$. On
383 the other hand, in the case of antibody effect, we obtain the total $S_{area} = 1775.83$ so that
384 $S_{avg} = 63.42$ with the effective average value of 98.66 sporozoites.

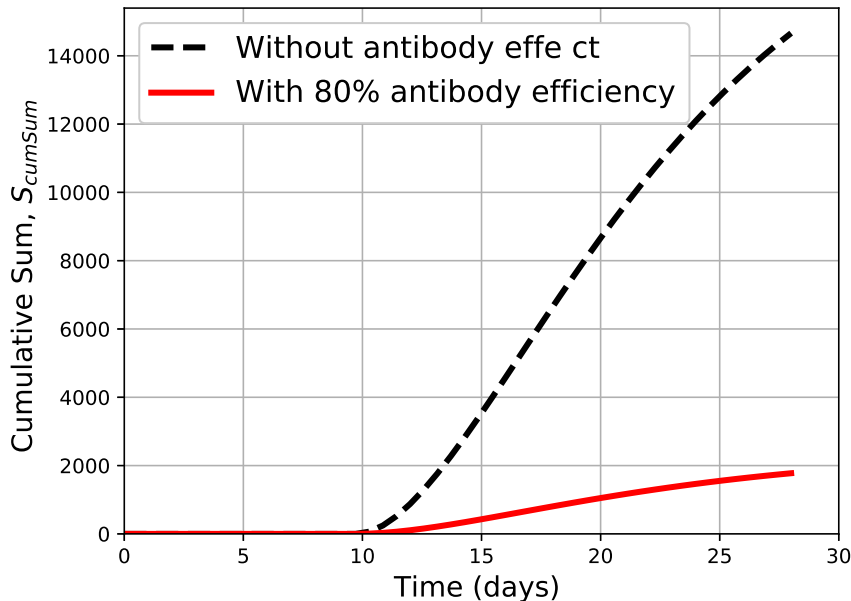


Figure 5: Plots of cumulative sums of sporozoite densities produced for model system (10) without any effect of human-antibodies, i.e. $\xi E_{a0} = 0$, and for the case with human-antibody effects, where $\xi = 80\%$, $E_{a0} = 11$ initial immune cells picked up in a blood meal. so that $\xi E_{a0} = 8.8$.

385 Next, we compute the cumulative sum of the sporozoite density up to time t , as the load
386 increases during the considered time frame. This cumulative sum is a sequence of partial sums
387 computed by partitioning time using a uniform step size and then numerically extracting the
388 densities of sporozoite (the sequences) from the solution curves 3e and 4d at the endpoints of
389 the partitioned time. We then use the function "cumsum" from the library "numpy" in Python
390 to plot the total sum of the extracted data up to time t . Plots of the cumulative sum of the
391 sporozoite densities showing their increase with time are shown in Figure 5. At the end of the
392 process for the considered time frame (28 days), the total cumulative sporozoite density in the
393 salivary gland of the feeding mosquito is $S_{area} = S_{cumsum}(28) = 24,500.88$ sporozoites for the
394 case where $\xi E_{a0} = 0$ (no antibody effect) and $S_{area} = S_{cumsum}(28) = 3921.83$ sporozoites for
395 the case where $\xi E_{a0} \neq 0$, a much smaller sum when antibody effects are considered. In all, the
396 cumulative sum of sporozoite density when $\xi E_{a0} \neq 0$, is much lower than that in the absence
397 of the action of antibodies in inhibiting fertilization.

3.2 Comparative and Sensitivity analyses of individual parameters and their combined effects on the model solution outcomes

400 Here, we investigate how individual parameters as well as a combination of parameters influence
401 the model solution, an outcome. The parameters to be considered are the immune-related

402 parameters ξ and $E_a(0)$, the initial number of ingested gametocytes G_{I0} and the fertilization
403 rate β_4 . Similar analyses for G_{I0} and β_4 were carried out in [71] in the absence of antibody effects,
404 where it was shown that when all other parameters were held fixed with a gametocyte sex ratio
405 of 0.25 used (i) higher sporozoite load corresponded to high numbers of ingested gametocytes
406 and the relationship was more than linear; and (ii) higher sporozoite load corresponded to
407 higher fertilization rate, although in this case, the relationship was less than linear. Moreover,
408 the combined effects of both G_{I0} and β_4 illustrated that control schemes that targeted both
409 parameters yielded a stronger positive impact. In particular, if $G_{I0} < 100$ regardless of how
410 high β_4 was or if $(G_{I0}, \beta_4) \in [0, 200] \times [0, 0.04]$, then a more desirable outcome in which less than
411 one oocyst was produced was observed. We now seek to replicate that study under immune
412 effects and begin by looking at the impacts of the individual variables.

413 **Sensitivity analysis of the individual impacts of the immune-related parameters: ξ** 414 **and $E_a(0)$**

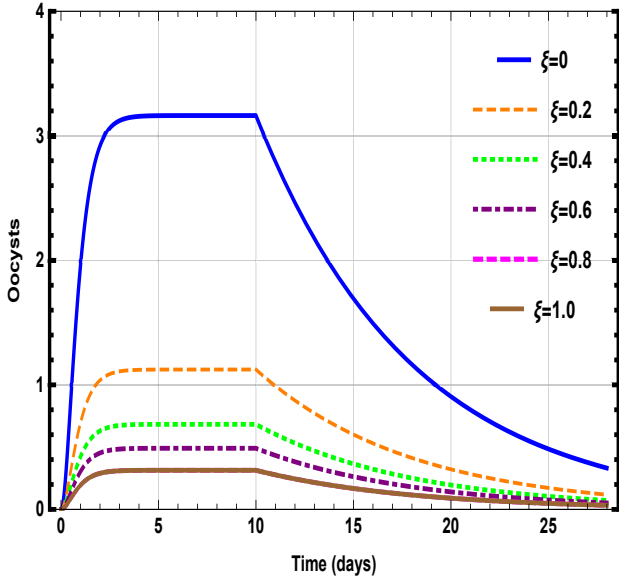
415 In this subsection, we investigate the effects of the immune-related parameters, ξ and $E_a(0)$, in
416 reducing the different parasite densities in the mosquitoes, with oocyst density and hence sporo-
417 zoite load key outputs, as well as the sensitivities of these outputs to changes in the individual
418 parameters. By sensitivity, we refer to the degree at which an input parameter influences the
419 model output, with sensitive parameters those which have a significant influence on the model
420 outcomes [32]. These analysis can help inform strategies aimed at controlling infectious diseases
421 [81, 83], and in our scenario the within-host parasite infection in the mosquito.

422 Figure 6 shows the oocyst densities and sporozoite loads as we vary the efficiency rate, ξ for
423 values in the set $\{0\%, 20\%, 40\%, 60\%, 80\%, 100\%\}$. The figure shows that as we increase ξ , the
424 oocyst densities and hence sporozoite loads both decrease. Thus oocyst density and sporozoite
425 loads are negatively correlated to human antibodies and thus the sensitivity index on oocyst
426 density and sporozoite load is negative. Moreover, it is easily seen that increasing ξ from 0 to
427 0.2 (20% increase), the peak oocyst is reduced by more than 60%.

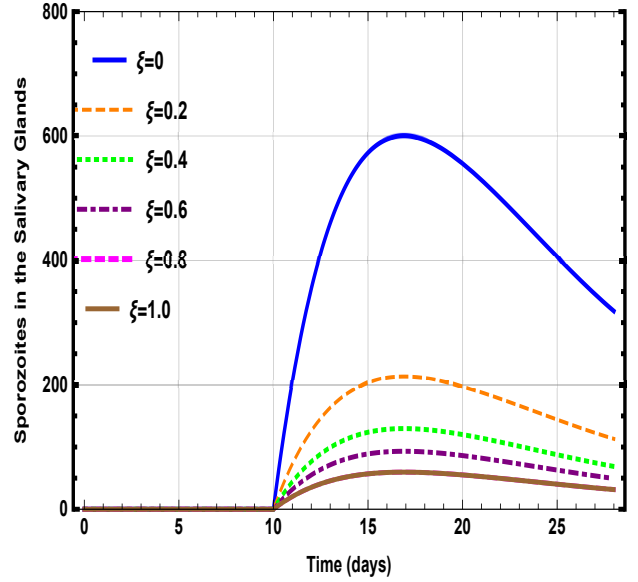
428 Next, in Figure 7, we vary the initial size of the ingested human antibodies, $E_a(0)$, that can
429 be picked up in a blood meal, while maintaining the efficiency ξ and all other parameters fixed at
430 the baseline values in Table 3 with the initial data as given in Table 11. Values of $E_a(0)$ are
431 selected from the set $\{0, 5, 11, 25\}$. As illustrated in Figure 7, the dynamics is similar to the
432 case of increasing ξ , whereby an increased number of ingested immune cells correlates with a
433 decrease in oocyst density and sporozoite load. What is strongly evident is that a high number
434 of immune cells need to be picked up to see a strong and desirable response with possibly the
435 production of less than 1 oocyst that can mature.

436 **Sensitivity analysis of the individual impacts of the number of ingested gametocytes** 437 **and fertilization rates under immune effects: G_0 and β_4**

438 Here, we investigate the sensitivity of the oocyst density to changes in both the size of the
439 number of ingested gametocytes and the fertilization rate, when human under immune factors
440 are in effect. We vary G_{I0} by selecting values from the set $\{100, 300, 600, 800, 1000\}$, a biological
441 feasible range as described in [71]. With $\tilde{m} = 0.25$, which is the proportion of gametocytes
442 that are males so that $1 - \tilde{m} = 0.75$ are females. Thus, for the stated G_{I0} , we have $mG_{I0} \in$
443 $\{25, 75, 100, 150, 200, 250\}$, and the plots are shown in Figure 8. The result when no immune
444 effectors were in effect was discussed in [71], where it was shown that the parameter which
445 had the greatest impact in sporozoite load reduction, under the stated conditions here, was the
446 initial number of gametocytes. In particular, even at a high fertilization rate, the number of
447 ingested gametocytes had a stronger influence on oocyst density, whereby for any $G_0 < 100$,
448 the number of generated oocyst was less than 1. Now, with antibody effects at the base levels

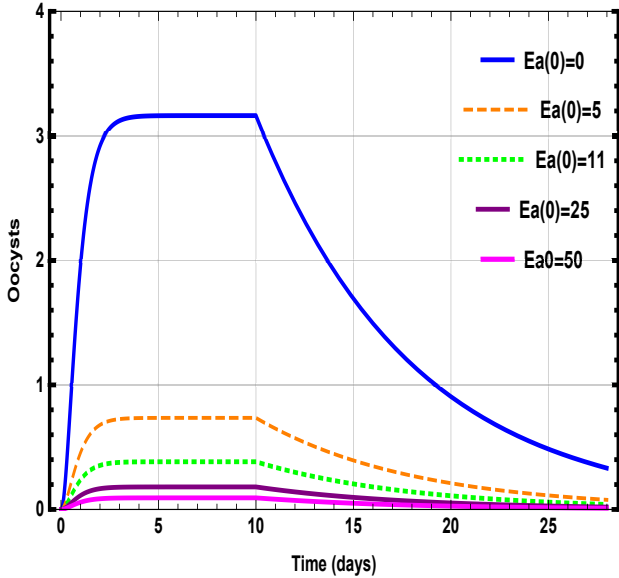


(a) Sensitivity of oocysts load to ξ

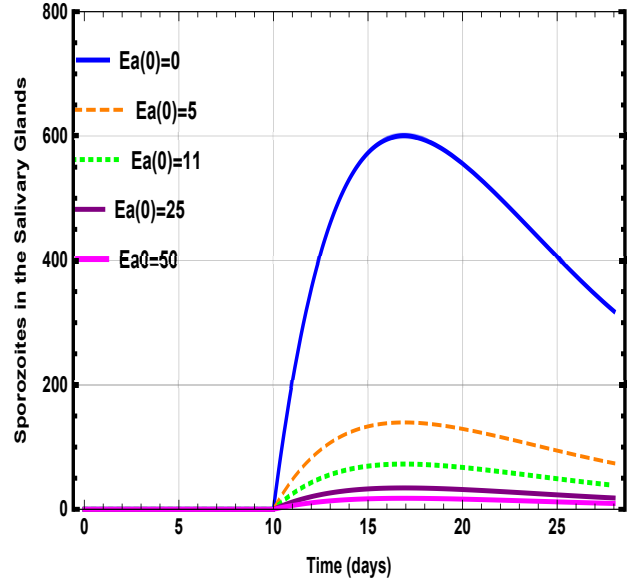


(b) sensitivity of sporozoites load to ξ

Figure 6: Plots of sensitivities of the response outputs for the number of oocysts and sporozoites as we vary ξ , choosing ξ values from the set $\{0\%, 20\%, 40\%, 60\%, 80\%, 100\%\}$, while maintaining the other parameters fixed as in Table 3. The figures show that antibodies have a positive impact in reducing oocyst density and sporozoite load. Notice that beyond 60% efficiency in antibody function, the reduction effect is not as drastic when compared with the effects at values of ξ higher than 60%.



(a) Oocysts for different values $E_a(0)$



(b) Sporozoites for different values $E_a(0)$

Figure 7: Sensitivity of solution curves of system (10) to changes in the initial values of the amount of human antibodies, $E_a(0)$, that can be ingested in a blood meal with all other parameters maintained at base values, as in Table 3. The initial values for the other state variables are held fixed as in Table 11. We vary $E_a(0)$ by using values in the set $\{0, 5, 11, 25\}$. We see that the higher the number of ingested human immune effectors the smaller the oocyst load and sporozoite density

449 chosen such that $\xi E_a(0) = 8.8$, we see that at higher levels of ingested initial gametocytes with
 450 a blood meal, the we can still achieve the desirable less than one oocyst, see Figure 8. That is,
 451 the antibody effects enhances the control such that a blood meal taken from an immune mature

452 humans in which the immune parameters are at the base levels as in Table 3, is less infectious
 453 than one of same size taken from a naive immune human. By less infectious, here we mean
 454 a blood meal that results in less than one oocyst production such that sporozoite production
 455 cannot occur.

456 In Figure 8, we look at how sensitive the solution curves of system (10) are to changes in
 457 the number of ingested gametocytes, G_{I0} , that can be picked with the blood meal, while in
 458 Figure 9, we look at sensitivities with respect to the fertilization rate between male and female
 459 gametes, β_4 , that can be picked with the blood meal. In Figure 8, we simulate the codes for
 460 values of $G_{I0} \in \{100, 300, 600, 800, 1000\}$ with the initial values defined by eqn. 11 for each
 461 chosen G_{I0} , while all parameters are set at the base parameters as defined in Table 3. The plots
 show that as we increase G_{I0} , the oocyst density and sporozoite load increase.

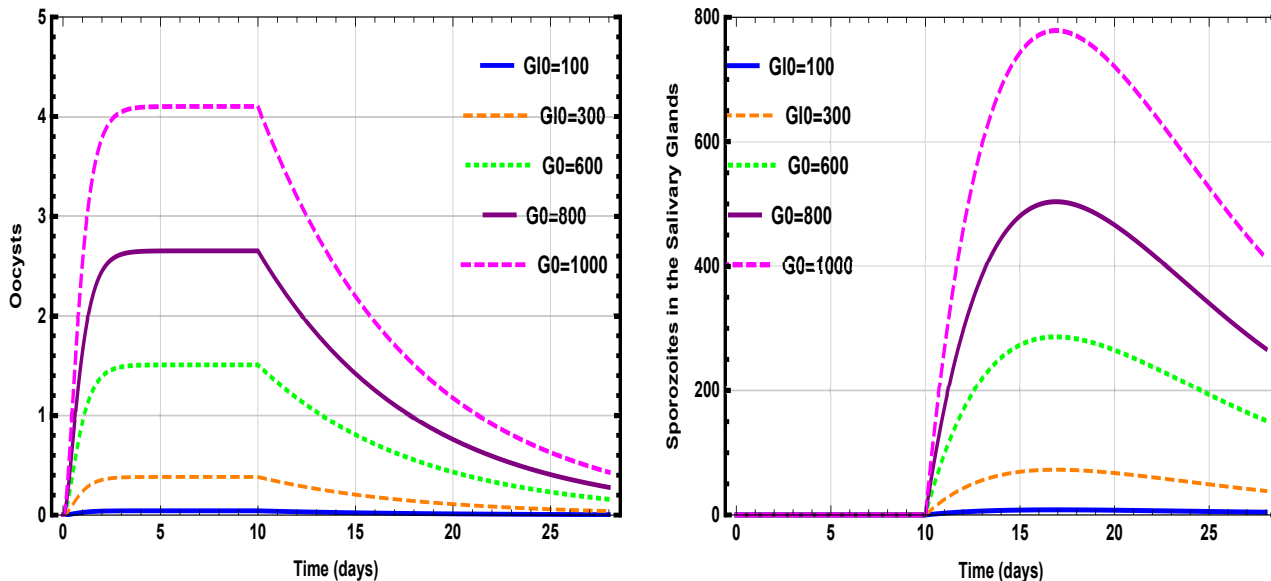


Figure 8: Solution trajectories showing the sensitivity of the model output (solution) to changes in G_{I0} , where G_{I0} varies through the values in the set $\{100, 300, 600, 800, 1000\}$. The plots show that as we increase G_{I0} , the oocyst density and sporozoite load increase.

462 Similarly, in Figure 9, the model is simulated for values of $\beta_4 \in \{0.02, 0.04, 0.06, 0.08, 0.1, 0.12, 0.14\}$
 463 with all parameters are set at the base parameters as defined in Table 3. The plots show similar
 464 increases in oocyst density and sporozoite load with increase in β_4 .
 465

466 **Sensitivity analysis of the combined impacts of fertilization rate and the number**
 467 **of ingested gametocytes under immune effects: G_0 and β_4**

468 We begin by looking at the contour plots for oocyst density as both fertilization rate, β_4 ,
 469 and the number of ingested gametocytes, G_{I0} , are varied. See Figure 10. Clearly, for any
 470 fixed G_{I0} , as fertilization rate increases the oocyst load increases. This is true regardless of
 471 immune effects. However, the immune effects is quite evident as the region in the (G_{I0}, β_4)
 472 space for which a density of less than 1 oocyst is produced on average is much larger, depicted
 473 by the brown region. If a larger percentage of gametocytes are ingested together with acquired
 474 immune effects taken to be the base value, then even with slightly higher fertilization rate, it
 475 is possible that the mosquito may not successfully become infectious, despite being infected.
 476 Our focus is on the oocyst density because it is more informative, as one oocyst on average
 477 implies the mosquito can be considered infectious as that one oocyst can produce 1000 to 10,000
 478 sporozoites upon bursting, after about 10 days. Thus, a control scheme aimed at reducing the
 479 size of G_{I0} and augmenting immune effectors picked up with reducing fertilization potential

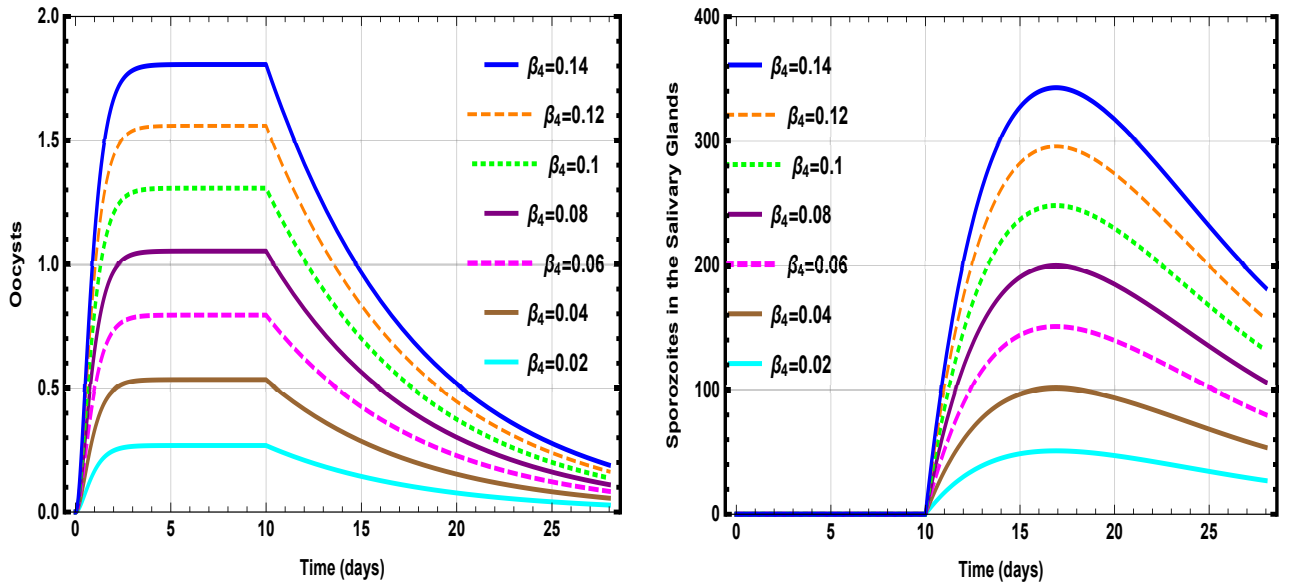


Figure 9: Solution trajectories showing the sensitivity of the model output (solution) to changes in β_4 , where β_4 varies through the values in the set $\{0.02, 0.04, 0.06, 0.08, 0.1, 0.14\}$. Likewise, as β_4 increases the oocyst density and sporozoite load both increase.

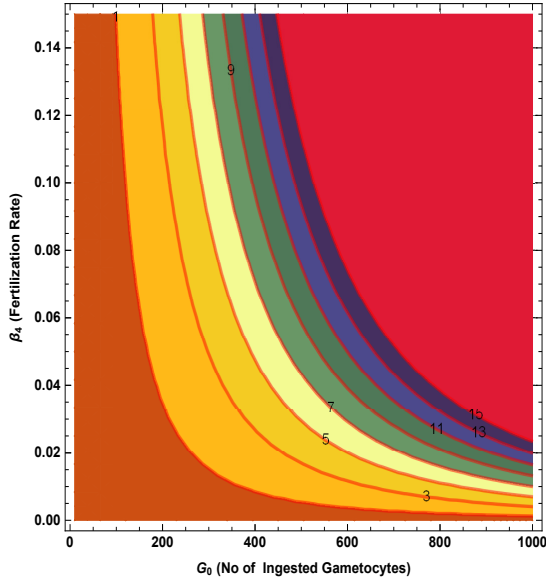
480 is quite desirable. This is even more important because the first two named strategies are
 481 strategies that can occur within the human. In particular, an infected human that seeks to
 482 complete their antimalarial treatment using non-fake drugs in a timely manner can help to
 483 reduce the gametocytes within the said human and hence reduce the potential for high number
 484 of gametocytes that can be picked up by a blood feeding mosquito on humans. Additionally,
 485 the use of a potential transmission blocking drug or vaccine administered to a human can help
 486 boost the humans' sexual-staged immune status and hence the size of ingested immune effectors,
 487 which can help diminish the fertilization potential of male and female gametes generated from
 488 the corresponding male and female gametocytes.

489 **Sensitivity analysis of the combined impacts of fertilization rate and immune-**
 490 **related parameters: β_4 , ξ and/or E_{a0} .**

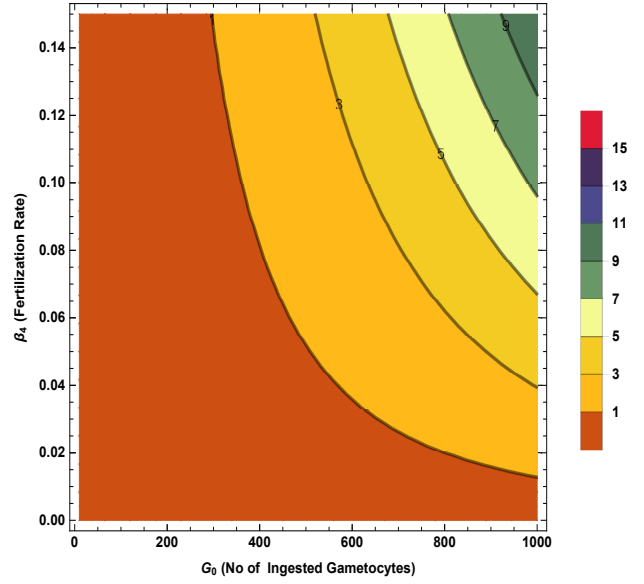
491 Here, we seek to understand the extent of the impact on oocyst density as we vary a pair of
 492 the model parameters from among β_4 , the fertilization rate, ξ the immune efficiency and E_{a0} ,
 493 the initial number of ingested human antibodies. We begin with β_4 versus ξ , their combined
 494 effect on oocyst density while E_{a0} is held fixed at a size of 11 immune Cells per blood meal
 495 (see Figure 11). As we vary both, we clearly see that even at the highest fertilization rate of
 496 $\beta_4 = 0.14$, an efficiency of 0.8 can render the biting mosquito eventually non-infectious with an
 497 average of less than one oocyst produced. Thus a control strategy that reduces both β_4 versus
 498 ξ , is desirable.

499 A similar result is obtained when we vary β_4 versus E_{a0} . In particular, we look at β_4 versus
 500 E_{a0} , their combined effects on oocyst density, while holding ξ fixed at two values 0.5 and 0.8 as
 501 shown in Figure 12. Comparing subfigures 12a and subfigures 12b, we see similar results that
 502 shows the regions in the (E_{a0}, β_4) space for which we have less than one average oocyst is larger
 503 for $\xi = 0.8$ (subfigure 12b) than for $\xi = 0.5$ (subfigure 12a). For $\xi = 0.8$ we can achieve less
 504 than 1 average oocyst even at the highest fertilization rate considered. Moreover, the control
 505 effort required for this latter case is less than the control effort for $\xi = 0.5$.

506 A more important comparative study, especially as it relates to transmission blocking drugs
 507 and/or vaccines, seems to be one that looks at oocyst load as a function of fertilization rate



(a) When $\xi E_{a0} = 0$, i.e. no immune effects.



(b) When we fix $\xi = 0.8$ and $E_{a0} = 11$.

Figure 10: Contour plot showing the average number of oocysts for different male and female gamete fertilization rates, β_4 , and number of gametocytes, G_0 , ingested with a blood meal. In subfigure 10a, there are no immune effects, meanwhile in subfigure 10b, we consider the baseline immune effects with all other parameters kept fixed as in Table 3.

508 β_4 and $\xi E_a(0)$, which gives the cumulative impact of antibodies in inhibiting fertilization of
 509 male and female gametes. The contour plots of the oocyst density is shown in Figure 13. The
 510 combined effect of $\xi E_a(0)$ is now convoluted in that a small $\xi E_a(0)$ value might mean that

- 511 (i) $E_a(0)$ is small and ξ is small so that $\xi E_a(0)$ is small;
- 512 (ii) ξ is small, closer to zero but $E_a(0)$ is not as large such that ξE_a is small, i.e. even though
 513 the initial density of $E_a(t)$ is large, the combined impact of $\xi E_a(0)$ is insignificant in
 514 reducing production of oocysts;
- 515 (iii) $E_a(0)$ is small and ξ is large, can be close to 1, but the fact $E_a(0)$ is small diminishes the
 516 combined effect of the product $\xi E_a(0)$ so that it is small.

517 From subfigure 13a, it is quite clear that for the cases when fertilization rate is quite high, the
 518 desirable impact of a small oocyst density (with a desirable density of less than one oocyst)
 519 can only potentially be achieved when $\xi E_a(0)$ is very large, say larger than 8. This is, if either
 520 ξ is close to one and $E_a(0)$ is much larger than 8 or ξ is small but $E_a(0)$ is much larger such
 521 that $\xi E_a(0)$ is larger than 8. Clearly at a fertilization rate of $\beta_4 = 0.8$ the $(\xi, E_a(0))$ region
 522 is depicted in subfigure 13b illustrated by the regions above the purple. This is for the case
 523 when the initial ingested gametocytes are maintained at base values. If we now look at the
 524 oocyst densities as we vary the dimensionless immune effect ξE_{a0} against the size of the initial
 525 numbers of ingested gametocytes, we see that when with fertilization rate β_4 is fixed at base
 526 value of 0.08 (subfigure 14a), the range of G_{10} varies that can be ingested for which we can
 527 have a less than one average oocyst is not that large. In fact, the desirable region with a less
 528 than one oocyst average increases but the increases is less than linear. A 50% reduction in
 529 fertilization rate to $\beta_4 = 0.04$ (subfigure 14b) provides a better results and larger region, but
 530 again the change is less than linear.

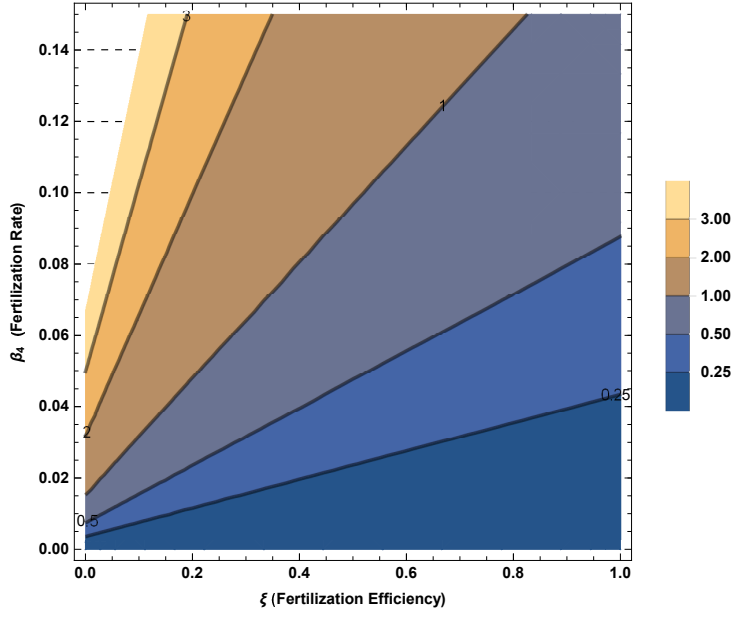


Figure 11: Contour plot of the average density of oocysts as fertilization rate, β_4 , and the efficiency of human-antibodies, ξ , are varied, for a fixed size of initial ingested gametocytes $E_a(0) = 11$. The remaining parameter values are fixed to at the baseline values as in Table 3.

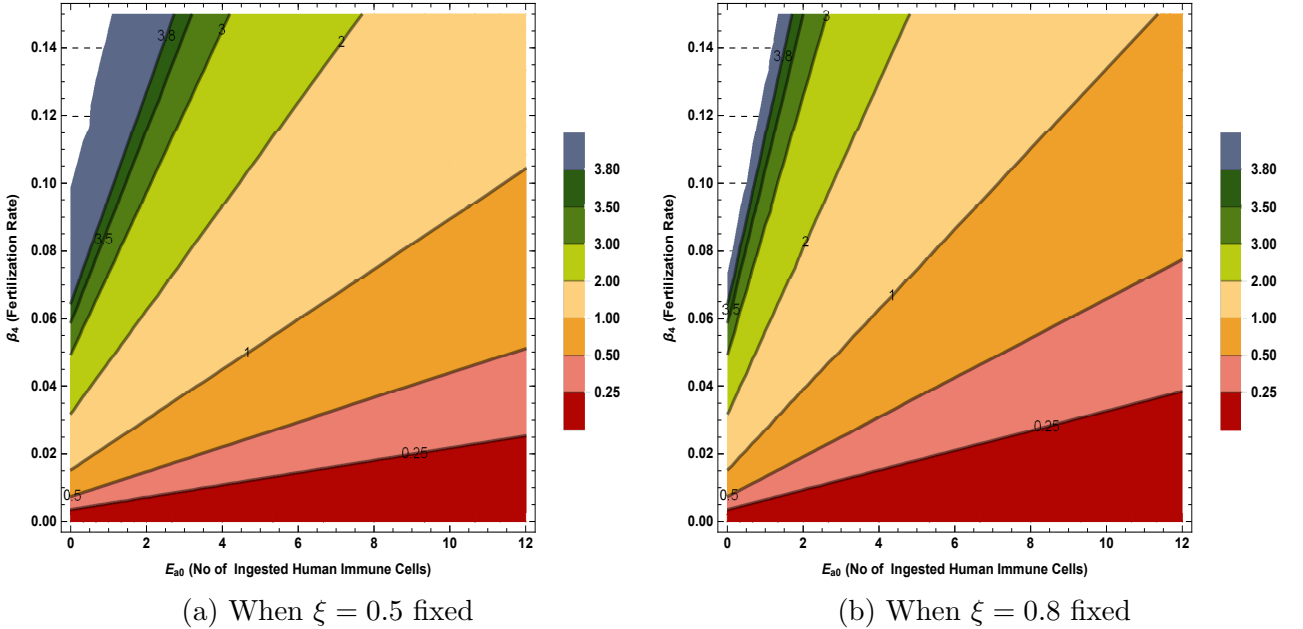
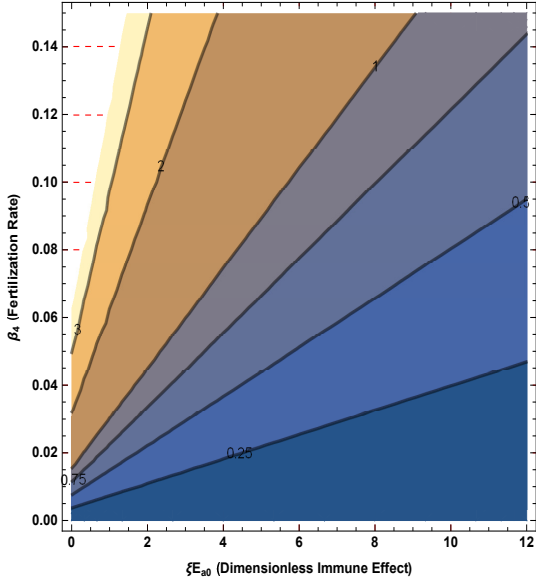
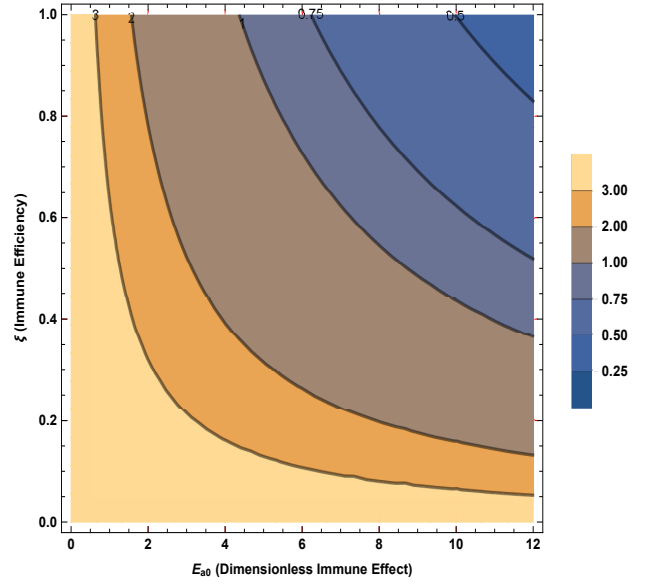


Figure 12: Contour plot of the average oocyst density as fertilization rate, β_4 , and the initial number of ingested human-antibodies, $E_a(0)$, are varied for $(E_{a0}, \beta_4) \in [0, 12] \times [0, 1.5]$, with ξ fixed, wher $\xi = 0.5$ is shown in subfigure 12a and $\xi = 0.8$ is shown in subfigure 12b. The remaining parameters are as given in Table 3.

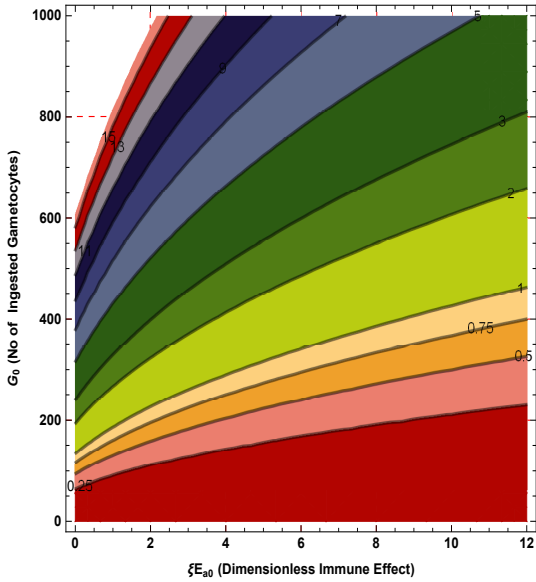


(a) β_4 versus the dimensionless immune effect ξE_{a0} .

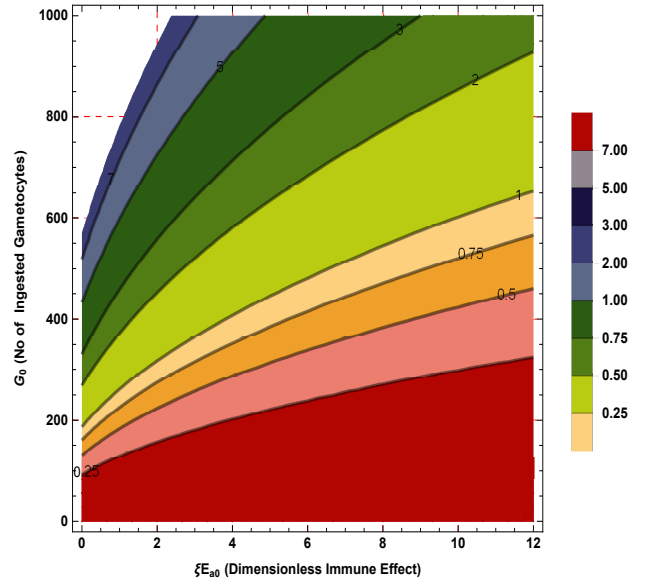


(b) ξ versus E_{a0} with β_4 held fixed.

Figure 13: Contour plots of the average oocyst density as (i) fertilization rate, β_4 , and the dimensionless immune effect ξE_{a0} are varied (subfigure 13a) and (ii) as ξ and E_{a0} are varied with $\beta_4 = 0.8$, held fixed (subfigure 13b). The remaining parameter values are as given in Table 3.



(a) β_4 versus the dimensionless immune effect ξE_{a0} with $\beta_4 = 0.08$.



(b) ξ versus E_{a0} with β_4 reduced by 50% to $\beta_4 = 0.04$.

Figure 14: Contour plots of the average oocyst density as the dimensionless immune effect ξE_{a0} is varied against the size of the initial numbers of ingested gametocytes with fertilization rate β_4 is fixed at 0.08 (subfigure 14a) and then reduced by 50% to 0.04 (subfigure 14b). The remaining parameter values are as given in Table 3.

4 Discussion of results

The work here is an extension of the work in [71], used to study through a mathematical model, the within mosquito-host life cycle of *Plasmodium falciparum* parasites under human immune effects. The model, a deterministic model, accounts for the developmental stage transformations of the within-mosquito dynamics of the malaria parasites from ingested gametocytes to sporozoites formation and seeks to illuminate the potential role of human antibodies that can be picked by a feeding mosquito during blood meal in inhibiting or slowing down the development of the parasite within the mosquito. The late stage (mature) gametocytes picked from the human were used as an input into the mosquito and initiated the within mosquito dynamics part the dynamics. The proposed model was mathematically shown to be well-posed in the sense that solutions exists, remain non-negative, are bounded and can be uniquely determined for a given parameter set. We numerically compared the simulations results for the cases when $E_{a0}\xi = 0$ (i.e. either $E_{a0} = 0$ or $\xi = 0$ or both are very small, hence no antibody effects) to the case when $\xi E_{a0} \neq 0$ (there is a human immune factor that can inhibit fertilization in the mosquito). In the latter case, $E_a(t)$ decays exponentially with time from its initial value \tilde{E}_{a0} , at the same rate as the rate at which the ingested human blood-meal disintegrates. Our results indicate that an sexual stage immunity response that elicits an efficient functional transmission blocking activity in the human can lower oocyst density and hence sporozoite load in a mosquito (see figures 3 and 4).

Figures 3 and 4 also illustrate that there is an overall dampening effect on the final outcome of the parasite development processes within the mosquito with immune factors considered. That is, increase in the size and efficiency of the antibodies in inhibiting fertilization leads to a decrease in the average oocyst density resulting in a lower sporozoite total load. We computed the cumulative sum of sporozoite density under the action of antibodies in inhibiting fertilization and compared it with the case when that was not so. With antibody effect, the cumulative sum was much lower (see figure 5). Both cumulative sums computed at end of 28 days yielded results that are within experimentally reported ranges, $1 \times 10^2 - 1 \times 10^5$, as noted in [8, 9]. Thus, TBI is a plausible way of blocking transmission; suppressing the development of sporozoites within a mosquito, which will in turn reduce the number in an infected mosquito that would be available for transmission to humans during a blood meal by the infected mosquito. These results highlight the fact that ongoing research on transmission blocking interventions (TBI) can potentially be quite promising. If control measures can be developed which incorporates factors within the human that could enhance the action of antibodies to disrupt the fertilization process and hence within-mosquito parasite development, there could be great gains in reducing transmission from mosquitoes to the humans. We note that these human immune factors must function efficiently in disrupting/inhibiting fertilization so that the end product is an average oocyst density that is less than one. A successful production of just one oocyst that eventually bursts to release sporozoite does not inhibit nor reduce the transmissibility potential of sporozoites from mosquitoes to humans since one oocyst can produce 1000 to 10,000 sporozoites [8, 71], which is undesirable if we intend to inhibit transmission from mosquitoes to humans.

Our numerical results highlight the fact that in understanding infectivity to mosquito, the key factors at play are the immune status of the individual from whom a blood meal is taken, the number of gametocytes ingested in a blood meal and hence the size of a blood meal, and the fertilization rate between male and female gametes that emerge via gametogenesis. Starting with gametocytes ingested, in Bousema et al. [13] and the associated references therein, it was noted that both the presence of mature gametocytes in the peripheral bloodstream and the human host immunity were determinant factors for a successful transmission of *P. falciparum* from a human to a mosquito. In a later field study conducted in three African countries by same author and collaborators [14], it was shown that there was a positive correlation between

580 mosquito gametocyte density and mosquito infection rates. On the other hand, in [37], it
 581 was shown that blood stage forms of malaria parasites decrease with age of individuals due to
 582 acquired immune effects against asexual stage parasites that develop with increases exposure
 583 to malaria. However, how the size of the asexual parasite forms correlate to gametocyte load
 584 and thus age, is not quite clear in general. For example in a cross sectional study in Burkina
 585 Faso [56], the authors showed that even though detection of gametocytes was more common in
 586 the children population, the percentage of asexual parasites that may then commit to develop
 587 into gametocytes may actually increase with age, which may weaken the correlation between
 588 high asexual forms and gametocyte load in both children and adults. The aforementioned
 589 highlight the complexity of malaria, a fact that is compounded by the known variability and
 590 heterogeneity that exists in parameters from field and laboratory studies, in addition to external
 591 influences, transmission settings and uncertainties around true parameter values. We believe
 592 our study thus play a significant role in that it can quantify the oocyst density regardless of
 593 the individual variations that exists. In particular, our results thus illuminates what outcomes
 594 can be observed under different scenarios of the studied parameter regime and under a wide
 595 parameter range as illustrated for fertilization rates, β_4 , and initial ingested gametocyte size
 596 G_{I0} . For example in figure 10 compared to subfigures 10a and 10b), we illustrated that we
 597 can have outcomes where a mosquito is potentially infected, regardless of the individual from
 598 which a blood meal is taken as long as a combination of parameters within feasible parameter
 599 ranges results in the said outcome. That is a blood meal from two separate individuals may
 600 yield different sizes of ingested gametocytes as well as different fertilization rates, but produce
 601 same oocysts density in a mosquito.

602 Next the immune response of the individual, which in this case refers to the sexual-staged
 603 immune response that can elicit transmission blocking activity in the mosquito that fed from
 604 the individual is important. In particular, a blood-meal that results in a small $E_a(0)$ value
 605 or a small $\xi E_a(0)$ value would not be desirable if high numbers of gametocytes are ingested
 606 with the blood meal. In this case, the potential for that blood meal to render the mosquito
 607 infectious would be dependent upon the number of gametocytes ingested and the fertilization
 608 rate between male and female gametes (see figure 10 and subfigure 13a). A blood meal that
 609 results in the baseline values of the sexual-staged immune effects would contribute to serve
 610 as some sort of a control, hence reducing the region in (G_{I0}, β_4) space over which the feeding
 611 mosquito can produce an average of about 1 or more oocysts (see figure 10b).

612 We note that in some studies, like the one in Malawi by the authors in [22], it was shown
 613 that the highest odds of having gametocytes when infected was among school aged children
 614 (5 – 15 years), when compared to adults (≥ 16 years) and under 5 years old children, who
 615 did not have a significant higher odds. Thus is it is clear that the inter-relationship between
 616 a human’s adaptive immune status (which is a function of age), the gametocyte load and the
 617 immune effectors against gametocytes ingested from an individual, is a more complex problem
 618 and may depend on the malaria region, whether the region under study is a high transmission
 619 region or low transmission region or whether malaria is all year round and stable (holoendemic)
 620 or whether it is seasonal as well as the blood type of the individuals [24]. In a study in [13]
 621 involving Tanzanian adults in an area where malaria transmission is seasonal but high, the
 622 authors noted that the adults under study had a lower exposure to gametocytes when they
 623 were compared to the children population. However, the authors asserted that the antibody
 624 specific to the sexual staged parasites would then be expected to decrease with age, rather
 625 than increase. With our results that illustrate that due to these antibody effects, humans with
 626 little sexual-staged immune response could be better mosquito infectors compared to those
 627 with sexual staged immune responses that can elicit a strong transmission blocking activity in
 628 the mosquito, the adult population who typically are the asymptomatic population may be a
 629 stronger reservoir of infection for malaria in many endemic regions, suggesting that they may

630 be better mosquito infectors overall. However, we understand that these results may be more
631 complex and one has to factor in the gametocyte load that is ingested in a blood meal, which
632 we have also shown to be a determinant of the density of oocysts produced but also the quality
633 of the gametocytes ingested, especially under adaptive immune pressure, how fecund they may
634 be. We believe that our results presented here in the form of contour plots that show variable
635 parameter spaces under which a mosquito could be infective is innovative and can be useful
636 and applicable in a wide variety of malaria settings.

637 In some sense, understanding the combined effect of ξE_{a0} in reducing oocysts load seems
638 more meaningful than studying each term individually. We did so in this manuscript. Some
639 questions worth exploring then are: Does age increase the functional efficiency of these immune
640 factors in inhibiting male and female gamete fertilization or not? In [13], where the authors
641 showed that the adults under study had a lower exposure to gametocytes when compared to the
642 children population but asserted that their sexual stage specific antibody would be expected
643 to decrease with age, rather than increase, compels us to ask: How does such a potential
644 decrease compare with the functional efficiency of the resulting antibody size? Or, in general,
645 how does size versus functional efficiency complement each other? Figures 13 and 14 show the
646 relationships of oocysts load to these key parameters and hence how they can impact mosquito
647 infectivity for different fertilization rates and gametocyte loads. What is strongly evident is
648 that a high number of immune cells need to be picked up to see a strong and desirable response
649 with possibly the production of less than 1 oocyst that can mature. It is worth noting that this
650 parameter is hard to characterize fully. However it leads to questions that experimentalists and
651 biologists can explore, which are (1) how many immune cells and types can be picked up by a
652 feeding mosquito during a blood meal? (2) Does the size of the immune effectors depend on the
653 human from which the blood meal is drawn? (3) Can the efficiency of the ingested immune cells
654 be quantified? If so, how? And these responses may differ in different transmission settings.

655 We believe that the work here can be beneficial to researchers developing further inves-
656 tigation so that its outcomes can help towards the current effort of developing transmission-
657 blocking-vaccines (TBV) and/or transmission-blocking-drugs (TBD). The efficacy of transmis-
658 sion blocking interventions are usually measured as either a reduction of the prevalence of
659 infected mosquitoes in field studies, or the reduction of oocyst density following membrane
660 feeding assays (considered to be gold standard) in laboratory studies [21, 20, 23, 77]. Our
661 results that mathematically show sensitivities to oocysts density to variations in densities of
662 ingested gametocytes, fertilization rate and immune effectiveness itself show the roles these
663 variables play as important determinants that should be accounted for when discussing efficacy
664 of transmission blocking intervention (TBI). Our model results can help to inform the determi-
665 nants of membrane feeding studies to assess the efficacy of transmission blocking intervention
666 in that we can quantify the number of oocysts produced after the intervention using antibodies.
667 With laboratory data for the different developmental stages of the parasite within the mosquito
668 fitted to our model, more specific predictions on the efficacy of such transmission blocking inter-
669 vention (TBI) strategies could be inferred. In particular, in our work we showed using contour
670 plots, how oocyst densities are affected for varied values of ingested gametocytes, fertilization
671 efficiency and immune effects. The results are directly tied to reduction in oocysts density but
672 can implicitly provide information on the prevalence of infected mosquitoes. For example, in
673 figures 8- 9, we showed how a reduction in ingested numbers of gametocytes in a blood meal is
674 correlated to a reduction in oocyst load in one mosquito, when we assume an efficacy of $\xi = 0.8$
675 and $E_a = 11$. Likewise, when we fix the size of the ingested gametocytes and allow these
676 immune effects to vary within each mosquito, higher efficiency and higher ingested immune
677 factors was linked to lower oocyst density (see figures 11 - 14) in each mosquito. However, if we
678 consider that different mosquitoes can ingest different densities of gametocytes in a blood meal,
679 otherwise identical in all other respects, then we can infer that prevalence will be higher if more

680 of the mosquitoes ingest higher densities of gametocytes. However, this is more complex as one
681 would have to consider the fertilization effects within each of these mosquitoes. As illustrated
682 in Figures 11(a) and (b), fertilization rate impacts oocyst density in a mosquito, where by a
683 reduction in oocyst density is observed even when high densities of gametocytes are ingested, as
684 long as fertilization rate is low. Thus although prevalence seems to be linked to oocyst density,
685 our results support the assertion that in general, transmission reducing interventions should
686 report reduction of infected intensity and prevalence. Additionally, one has to be cautious as
687 to what this might mean for possible infection to humans. In [21], it was shown that mosquito
688 parasite load had a per bite influence on the probability of mosquito-to-human transmission,
689 with malaria infection to vaccinated humans highly probable when the feeding mosquito had
690 > 1000 residual-sporozoites in its salivary glands. In addition to oocysts intensity, sporozoite
691 load are important output functions.

692 5 Conclusions

693 Malaria control strategies that focus on the use of insecticide treated bednets (ITNS), effective
694 antimalarial drugs and control of mosquito populations are yielding some success in the field
695 towards malaria control. However, even with the observed gains, malaria deaths are still high
696 and the number of cases are still high. Additionally, compliance with regards to using and
697 sleeping under ITNs as well anti-malarial drug resistance spread and insecticide resistance
698 continue to complicate and make control challenging. Thus, development of effective malaria
699 control strategies that can utilize human factors, such as the human immune effectors developed
700 during within-human parasitemia, that would work to inhibit parasite development progress
701 within the mosquito that fed from that human, continue to be desirable. Additional factors
702 such as transmission blocking vaccines or transmission blocking drugs are also desirable and
703 are also under investigation [11, 16, 78]. These methods aim to exploit the human-parasite-
704 mosquito-human interaction as well as the fact that humans can be given these vaccines and/or
705 drugs to target the parasite within the mosquito, hence disrupting the parasite life-cycle and
706 potentially disrupting successful transmission between humans and mosquitoes. Our results
707 demonstrates that efforts geared towards this form of malaria control methodology, aimed at
708 disrupting the malaria parasite life cycle in a mosquito can produce promising and desirable
709 results. Moreover, if combined with the other malaria control methodologies, then a significant
710 reduction in the morbidity and mortality or malaria among the hardest hit regions could be
711 achieved, with malaria eradication a possibility.

712 The true nature and mechanism of the function of the human antibodies within the mosquito
713 gut as well as the transition time and rate from sporoblast formation to presence of sporozoites
714 in the salivary glands of the mosquito system remain to be investigated. It is also not clear to
715 us if a mosquito can harbour different strains of the parasite in different stages of development
716 or if there is selective development once a mosquito is infected. These are important questions
717 that can affect the nature of the growth processes modeled in this manuscript.

718 Our model is a deterministic model, where the threshold of one oocyst production is defined
719 as an effective transmission blocking activity. However, a further adaptation of the model
720 could include a stochastic formulation in which we use probabilistic analysis to define the
721 threshold parameter, whereby transmission blocking efficacy is defined as the probability that
722 a mosquito is infected with oocyst versus not infected. This would be pursued in future studies.
723 Furthermore, a comprehensive study that starts from the within human parasite levels to the
724 mosquito parasite levels can help illuminate how human factors under a varied conditions can
725 impact oocyst density and sporozoite load and hence disease prevalence.

Acknowledgment

WA Woldegerima acknowledge the support from the DST/NRF SARChI Chair in Mathematical Models and Methods in Biosciences and Bioengineering at the University of Pretoria, grant No. 82770, and National Science Centre of Poland, grant 2017/25/B/ST1/00051. MIT-E acknowledges the support of Lehigh University and GAN acknowledges the grants and support of the University of Buea, Cameroon and the Hochschule Mittweida University of Applied Sciences, Germany. GAN also acknowledges the Cameroonian Ministry of Higher Education through the initiative for the modernization of research in Cameroon’s Higher Education. All authors also acknowledge the sponsorship of the Commission for Developing Countries (CDC) in conjunction with the International Mathematics Union (IMU) through the CDC-ADMP (African Diaspora Mathematicians Program) grant that made it possible for interactive collaborative work that lead to some of the work. MIT-E also acknowledges support via NSF grant 1815912 which enabled her engagement in completing the project.

Conflict of Interest

All authors declare no potential conflict of interest.

References

1. F.K. Acquah, J. Adjah, K.C. Williamson, and L.E. Amoah. Transmission-blocking vaccines: old friends and new prospects. *Infect Immun*, 87(6):e00775–18, 2019. 3, 4
2. MASAMICHI AIKAWA, JOAN RENER, RICHARD CARTER, and LOUIS H MILLER. An electron microscopical study of the interaction of monoclonal antibodies with gametes of the malarial parasite plasmodium gallinaceum. *Journal of Eukaryotic Microbiology*, 28(3):383–388, 1981. 12, 14
3. Ahmed SI Aly, Ashley M Vaughan, and Stefan HI Kappe. Malaria parasite development in the mosquito and infection of the mammalian host. *Annual review of microbiology*, 63:195–221, 2009. 2, 5, 6, 8
4. Roumen Anguelov, Yves Dumont, and Jean Lubuma. Mathematical modeling of sterile insect technology for control of anopheles mosquito. *Computers & Mathematics with Applications*, 64(3):374–389, 2012. 4
5. Myriam Arévalo-Herrera, Yezid Solarte, Catherin Marin, Mariana Santos, Jenniffer Castellanos, John C Beier, and Sócrates Herrera Valencia. Malaria transmission blocking immunity and sexual stage vaccines for interrupting malaria transmission in latin america. *Memórias do Instituto Oswaldo Cruz*, 106:202–211, 2011. 2
6. Alison Deckhut Augustine, B Fenton Hall, Wolfgang W Leitner, Annie X Mo, Tonu M Wali, and Anthony S Fauci. Niaid workshop on immunity to malaria: addressing immunological challenges. *Nature immunology*, 10(7):673–678, 2009. 2
7. WR Ballou. The development of the rts, s malaria vaccine candidate: challenges and lessons. *Parasite immunology*, 31(9):492–500, 2009. 3
8. Luke A Baton and Lisa C Ranford-Cartwright. Spreading the seeds of million-murdering death: metamorphoses of malaria in the mosquito. *Trends in parasitology*, 21(12):573–580, 2005. 2, 3, 5, 6, 7, 8, 14, 24

- 766 9. John C Beier. Malaria parasite development in mosquitoes. *Annual review of entomology*,
767 43(1):519–543, 1998. 2, 8, 24
- 768 10. Sandra Bennink, Meike J. Kiesow, and Gabriele Pradel. The development of malaria
769 parasites in the mosquito midguto. *Cellular microbiology*, 18(7):905–918, 2016. 2
- 770 11. Sumi Biswas. Can we block malaria transmission. [https://www.ndm.ox.ac.uk/
771 sumi-biswas-can-we-block-malaria-transmission](https://www.ndm.ox.ac.uk/sumi-biswas-can-we-block-malaria-transmission), 2017. Accessed: March 30, 2021.
772 3, 27
- 773 12. A.M. Blagborough, T.S. Churcher, L.M. Upton, A.C. Ghani, P.W. Gething, and R.E.
774 Sinden. Transmission-blocking interventions eliminate malaria from laboratory popula-
775 tions. *Nature Communications*, 4(9):1812, 2012. 10
- 776 13. J.T. Bousema, C.J. Drakeley, J. Kihonda, J.C.M. Endriks, N.I.J. Akim, W. Roeffen, and
777 R.W. Sauerwein. A longitudinal study of immune responses to plasmodium falciparum
778 sexual stage antigens in tanzanian adults. *Parasite Immunology*, 29(6):309–317, 2007. 3,
779 24, 25, 26
- 780 14. T. Bousema, C. J. Sutherland, T. S. Churcher, B. Mulder, L. C. Gouagna, E. M. Riley,
781 G. A. Targett, and C. J. Drakeley. Human immune responses that reduce the transmission
782 of plasmodium falciparum in african populations. *International journal for parasitology*,
783 41(3-4):293–300, 2011. 10, 24
- 784 15. Teun Bousema, Colin J Sutherland, Thomas S Churcher, Bert Mulder, Louis C Gouagna,
785 Eleanor M Riley, Geoffrey AT Targett, and Chris J Drakeley. Human immune responses
786 that reduce the transmission of plasmodium falciparum in african populations. *Interna-
787 tional journal for parasitology*, 41(3):293–300, 2011. 2, 3, 7
- 788 16. Richard Carter. Transmission blocking malaria vaccines. *Vaccine*, 19(17):2309–2314,
789 2001. 3, 27
- 790 17. CDC. Anopheles mosquitoes. [https://www.cdc.gov/malaria/about/biology/
791 mosquitoes/](https://www.cdc.gov/malaria/about/biology/mosquitoes/), 2015. reviewed and updated: October 21, 2015, Last Accessed: August
792 30, 2017. 2
- 793 18. Neha Chaturvedi, Praveen K Bharti, Archana Tiwari, and Neeru Singh. Strategies &
794 recent development of transmission-blocking vaccines against plasmodium falciparum.
795 *The Indian journal of medical research*, 143(6):696, 2016. 3, 4
- 796 19. Lauren M Childs and Olivia F Prosper. Simulating within-vector generation of the
797 malaria parasite diversity. *PloS one*, 12(5):e0177941, 2017. 4
- 798 20. Thomas S Churcher, Andrew M Blagborough, Michael Delves, Chandra Ramakrishnan,
799 Melissa C Kapulu, Andrew R Williams, Sumi Biswas, Dari F Da, Anna Cohuet, and
800 Robert E Sinden. Measuring the blockade of malaria transmission—an analysis of the
801 standard membrane feeding assay. *International journal for parasitology*, 42(11):1037–
802 1044, 2012. 2, 3, 26
- 803 21. Thomas S Churcher, Robert E Sinden, Nick J Edwards, Ian D Poulton, Thomas W
804 Rampling, Patrick M Brock, Jamie T Griffin, Leanna M Upton, Sara E Zakutansky,
805 Katarzyna A Sala, et al. Probability of transmission of malaria from mosquito to human
806 is regulated by mosquito parasite density in naive and vaccinated hosts. *PLoS pathogens*,
807 13(1):e1006108, 2017. 26, 27

- 808 22. Jenna E. Coalson, Jenny A. Walldorf, Lauren M. Cohee, Miriam D. Ismail, Don Math-
809 anga, Regina Joice Cordy, Matthias Marti, Terrie E. Taylor, Karl B. Seydel, Miriam K.
810 Laufer, and Mark L. Wilson. High prevalence of plasmodium falciparum gametocyte
811 infections in school-age children using molecular detection: patterns and predictors of
812 risk from a cross-sectional study in southern malawi. *Malaria Journal*, 15(1):527, 2016.
813 25
- 814 23. Dari F Da, Thomas S Churcher, Rakiswendé S Yerbanga, Bienvenue Yaméogo, Ibrahim
815 Sangaré, Jean Bosco Ouedraogo, Robert E Sinden, Andrew M Blagborough, and Anna
816 Cohuet. Experimental study of the relationship between plasmodium gametocyte den-
817 sity and infection success in mosquitoes; implications for the evaluation of malaria
818 transmission-reducing interventions. *Experimental parasitology*, 149:74–83, 2015. 26
- 819 24. RM de Jong, SK Tebeje, L MeersteinKessel, FG Tadesse, MM Jore, W Will Stone, and
820 T Bousema. Immunity against sexual stage plasmodium falciparum and plasmodium
821 vivax parasites. *Immunol Rev.*, 293(1):190–215, 2020. 3, 25
- 822 25. MJ Delves, F Angrisano, and AM Blagborough. Antimalarial transmission-blocking
823 interventions: past, present, and future. *Trends in parasitology*, 34(9):735–746, 2018. 2,
824 3, 4
- 825 26. Ravi Dhar and Nirbhay Kumar. Role of mosquito salivary glands. *CURRENT SCIENCE-*
826 *BANGALORE-*, 85(9):1308–1313, 2003. 2
- 827 27. Ogobara K Doumbo, Karamoko Niaré, Sara A Healy, Issaka Sagara, and Patrick E Duffy.
828 Malaria transmission-blocking vaccines: present status and future perspectives. *Towards*
829 *Malaria Elimination-A Leap Forward*, 2018. 3, 4
- 830 28. S. J. Draper, B. K. Sack, C. R. King, C. M. Nielsen, J. C. Rayner, M. K. Higgins, C. A.
831 Long, and R. A. Seder. Malaria vaccines: Recent advances and new horizons. *Cell host*
832 *& microbe*, 24(1):43–56, 2018. 3
- 833 29. Donald L Gardiner and Katharine R Trenholme. Plasmodium falciparum gametocytes:
834 playing hide and seek. *Annals of translational medicine*, 3(4), 2015. 3
- 835 30. Ricardo T Gazzinelli, Parisa Kalantari, Katherine A Fitzgerald, and Douglas T Golen-
836 bock. Innate sensing of malaria parasites. *Nature Reviews Immunology*, 14(11):744–757,
837 2014. 2
- 838 31. Patricia M Graves and Hellen Gelband. Vaccines for preventing malaria (pre-
839 erythrocytic). *The Cochrane database of systematic reviews*, 2016(4):CD006198, 2006.
840 3
- 841 32. DM Hamby. A review of techniques for parameter sensitivity analysis of environmental
842 models. *Environmental monitoring and assessment*, 32(2):135–154, 1994. 17
- 843 33. S.I. Hay, D.L. Smith, and R.W. Snow. Measuring malaria endemicity from intense to
844 interrupted transmission. *The Lancet. Infectious diseases*, 84(6):369–378, 2008. 11
- 845 34. Adrian VS Hill. Vaccines against malaria. *Philosophical Transactions of the Royal Society*
846 *B: Biological Sciences*, 366(1579):2806–2814, 2011. 3
- 847 35. Lauren E. Holz, Daniel Fernandez-Ruiz, and William R Heath. Protective immunity to
848 liver-stage malaria. *Clinical & Translational Immunology*, 5:e105, 2016. 2

- 849 36. Po-Fang Hsieh and Yasutaka Sibuya. *Basic theory of ordinary differential equations*.
850 Springer Science & Business Media, 2012. 39
- 851 37. Rodriguez-Barraquer I, Arinaitwe E, Jagannathan P, Kanya MR, Rosenthal PJ, Rek J,
852 Dorsey G, Nankabirwa J, Staedke SG, Kilama M, Drakeley C, Ssewanyana I, Smith DL,
853 and Greenhouse B. Quantification of anti-parasite and anti-disease immunity to malaria
854 as a function of age and exposure. *Elife*, 7:e35832, 2018. 25
- 855 38. Melissa C Kapulu, Sumi Biswas, Andrew Blagborough, Sarah C Gilbert, Robert E Sin-
856 den, and Adrian VS Hill. Viral vectored transmission blocking vaccines against plasmodium
857 falciparum. *Malaria Journal*, 9(2):O22, 2010. 3
- 858 39. David C Kaslow. Transmission-blocking immunity against malaria and other vector-
859 borne diseases. *Current opinion in immunology*, 5(4):557–565, 1993. 2
- 860 40. DC Kaushal, R Carter, LH Miller, and G Krishna. Gametocytogenesis by malaria para-
861 sites in continuous culture. *Nature*, 286(5772):490–492, 1980. 2
- 862 41. Jonas A Kengne-Ouafo, Colin J Sutherland, Fred N Binka, Gordon A Awandare, Britta C
863 Urban, and Bismarck Dinko. Immune responses to the sexual stages of plasmodium
864 falciparum parasites. *Frontiers in immunology*, 10:136, 2019. 2, 3
- 865 42. E Klein, D Smith, MF Boni, and R Laxminarayan. Clinically immune hosts as a refuge
866 for drug-sensitive malaria parasites. *Malar J*, 7(1):67, 2008. 2
- 867 43. Antoniana U Krettli and Louis H Miller. Malaria: a sporozoite runs through it. *Current*
868 *Biology*, 11(10):R409–R412, 2001. 2
- 869 44. Andrea Kuehn and Gabriele Pradel. The coming-out of malaria gametocytes. *BioMed*
870 *Research International*, 2010, 2010. 3
- 871 45. Matthew B Laurens. RTS, S/AS01 vaccine (Mosquirix™): An overview. *Human Vac-*
872 *cines & Immunotherapeutics*, 16(3):480–489, 2020. 3
- 873 46. Carrie A. Manore, Miranda I. Teboh-Ewungkem, Olivia Prosper, Angela Peace,
874 Katharine Gurski, and Zhilan Feng. Intermittent preventive treatment (ipt): Its role
875 in averting disease-induced mortality in children and in promoting the spread of resis-
876 tance spread in areas with population movement antimalarial drug resistance. *Bull Math*
877 *Biol*, 81:193–234, 2019. 2, 11
- 878 47. Philip G McQueen, Kim C Williamson, and F Ellis McKenzie. Host immune con-
879 straints on malaria transmission: insights from population biology of within-host para-
880 sites. *Malaria journal*, 12(1):1, 2013. 3, 7
- 881 48. Ann-Kristin Mueller, Florian Kohlhepp, Christiane Hammerschmidt, and Kristin Michel.
882 Invasion of mosquito salivary glands by malaria parasites: prerequisites and defense
883 strategies. *International journal for parasitology*, 40(11):1229–1235, 2010. 2
- 884 49. Gideon A Ngwa. On the population dynamics of the malaria vector. *Bulletin of mathe-*
885 *matical biology*, 68(8):2161–2189, 2006. 4
- 886 50. Gideon A Ngwa and William S Shu. A mathematical model for endemic malaria with
887 variable human and mosquito populations. *Mathematical and computer modelling*, 32(7-
888 8):747–764, 2000. 4

- 889 51. Gideon A Ngwa and Miranda I Teboh-Ewungkem. A mathematical model with quaran-
890 tine states for the dynamics of ebola virus disease in human populations. *Computational*
891 *and mathematical methods in medicine*, 2016, 2016. 4
- 892 52. Gideon A Ngwa, Miranda I. Teboh-Ewungkem, Yves Dumont, Rachid Ouifki, and Jacek
893 Banasiak. On a three-stage structured model for the dynamics of malaria transmission
894 with human treatment, adult vector demographics and one aquatic stage. *Theoretical*
895 *Biology*, 481(21):202–222, 2019. 11
- 896 53. Gideon A Ngwa, Terence T. Wankah, Mary Y. Fomboh-Nforba, Calsitus N. Ngonghala,
897 and Miranda I. Teboh-Ewungkem. On a reproductive stage-structured model for the
898 population dynamics of the malaria vector. *Bulletin of Mathematical Biology*, 76:2476–
899 2516, 2014. 11
- 900 54. Gideon A Ngwa, Woldegebriel A Woldegerima, and Miranda I Teboh-Ewungkem. A
901 mathematical study of the implicit role of innate and adaptive immune responses on
902 within-human plasmodium falciparum parasite levels. *Journal of Biological Systems*,
903 28(2):377–429, 2020. 2, 3
- 904 55. Julia K Nunes, Colleen Woods, Terrell Carter, Theresa Raphael, Merribeth J Morin,
905 Diadier Diallo, Didier Leboulleux, Sanjay Jain, Christian Loucq, David C Kaslow, et al.
906 Development of a transmission-blocking malaria vaccine: progress, challenges, and the
907 path forward. *Vaccine*, 32(43):5531–5539, 2014. 3
- 908 56. A. L. Ouédraogo, T. Bousema, S. J. de Vlas, N. Cuzin-Ouattara, J. P. Verhave, C. Drake-
909 ley, A. J. Luty, and R. Sauerwein. The plasticity of plasmodium falciparum gametocy-
910 taemia in relation to age in burkina faso. *Malaria journal*, 9:281, 2010. 25
- 911 57. A. L. Ouédraogo, W. Roeffen, S. J. Luty, A. J. and de Vlas, I. Nebie, E. Ilboudo-Sanogo,
912 N. Cuzin-Ouattara, K. Teleen, A. B. Tiono, S. B. Sirima, J. P. Verhave, T. Bousema, and
913 R. Sauerwein. Naturally acquired immune responses to plasmodium falciparum sexual
914 stage antigens pfs48/45 and pfs230 in an area of seasonal transmission. *Infection and*
915 *immunity*, 79(12):4957–4964, 2011. 10, 11
- 916 58. MVI PATH. The rts,s malaria vaccine candidate. [http://www.malariavaccine.org/
917 sites/www.malariavaccine.org/files/content/page/files/mviCVIA_rtss.pdf](http://www.malariavaccine.org/sites/www.malariavaccine.org/files/content/page/files/mviCVIA_rtss.pdf),
918 2017. Published: April 2017, Accessed: November, 2017. 3
- 919 59. Gaston Pichon, HP Awono-Ambene, and Vincent Robert. High heterogeneity in the
920 number of plasmodium falciparum gametocytes in the bloodmeal of mosquitoes fed on
921 the same host. *Parasitology*, 121(2):115–120, 2000. 14
- 922 60. J. Renner, R. Carter, Y. Rosenberg, and L.H. Miller. Anti-gamete monoclonal anti-
923 bodies synergistically block transmission of malaria by preventing fertilization in the
924 mosquito. *Proceedings of the National Academy of Sciences of the United States of Amer-*
925 *ica*, 77(11):6797–6799, 1980. 14
- 926 61. RW Sauerwein and T Bousema. Transmission blocking malaria vaccines: Assays and
927 candidates in clinical development. *Vaccine*, 33(52):7476–7482, 2015. 3
- 928 62. A. SAUL. Efficacy model for mosquito stage transmission blocking vaccines for malaria.
929 *Parasitology*, 135(13):1497–1506, 2008. 10
- 930 63. Robert Sinden. A biologist’s perspective on malaria vaccine development. *Human vac-*
931 *cines*, 6(1):3–11, 2010. 2

- 932 64. Robert E Sinden. Developing transmission-blocking strategies for malaria control. *PLoS*
933 *Pathogens*, 13(7), 2017. 5
- 934 65. J.C. Tavares. *Malaria*. Colloquium Series on Integrated Systems Physiology: From
935 Molecule to Function. Biota Publishing, 2013. 2
- 936 66. Miranda I Teboh-Ewungkem, Jemal Mohammed-Awel, Frederick N Baliraine, and
937 Scott M Duke-Sylvester. The effect of intermittent preventive treatment on anti-malarial
938 drug resistance spread in areas with population movement. *Malaria journal*, 13(1):428,
939 2014. 2, 11
- 940 67. Miranda I. Teboh-Ewungkem, Gideon A Ngwa, and Mary Y. Fomboh-Nforba. A
941 multistage mosquito-centered mathematical model for malaria dynamics that captures
942 mosquito gonotrophic cycle contributions to its population abundance and malaria trans-
943 mission, 2019. 11
- 944 68. Miranda I Teboh-Ewungkem, Gideon A Ngwa, and Calistus N Ngonghala. Models and
945 proposals for malaria: a review. *Mathematical Population Studies*, 20(2):57–81, 2013. 4
- 946 69. Miranda I Teboh-Ewungkem, Olivia Prosper, Katharine Gurski, Carrie A Manore, An-
947 gela Peace, and Zhilan Feng. Intermittent preventive treatment (ipt) and the spread of
948 drug resistant malaria. In *Applications of Dynamical Systems in Biology and Medicine*,
949 pages 197–233. Springer, 2015. 11
- 950 70. Miranda I Teboh-Ewungkem and Miao Wang. Male fecundity and optimal gametocyte
951 sex ratios for plasmodium falciparum during incomplete fertilization. *Journal of theoret-*
952 *ical biology*, 307:183–192, 2012. 3, 4, 12
- 953 71. Miranda I Teboh-Ewungkem and Thomas Yuster. A within-vector mathematical model
954 of plasmodium falciparum and implications of incomplete fertilization on optimal game-
955 tocyte sex ratio. *Journal of theoretical biology*, 264(2):273–286, 2010. 2, 3, 4, 5, 6, 7, 8,
956 10, 11, 12, 14, 17, 24, 34
- 957 72. Miranda I Teboh-Ewungkem and Thomas Yuster. Evolutionary implications for the
958 determination of gametocyte sex ratios under fecundity variation for the malaria parasite.
959 *Journal of Theoretical Biology*, 408:260–273, 2016. 3, 4
- 960 73. Miranda I Teboh-Ewungkem, Thomas Yuster, and Nathaniel H Newman. A mathe-
961 matical model of the within-vector dynamics of the plasmodium falciparum protozoan
962 parasite, 2010. 2, 3, 4, 6, 8, 10, 34
- 963 74. Manasa Valupadasu and Uday Mateti. Advanced malarial vaccines: A promising ap-
964 proach in the treatment of malaria. *Systematic Reviews in Pharmacy*, 3(1):31, 2012.
965 3
- 966 75. J.M. Vinetz. Plasmodium ookinete invasion of the mosquito midgut. In *Compans, R.W.*
967 *et al. (eds) Malaria: Drugs, Disease and Post-genomic Biology. Current Topics in Micro-*
968 *biology and Immunology*, volume 295, pages 357–382. Springer, Berlin, Heidelberg, 2005.
969 8
- 970 76. Ishan Wadi, Anupkumar R Anvikar, Mahendra Nath, C Radhakrishna Pillai, Abhinav
971 Sinha, and Neena Valecha. Critical examination of approaches exploited to assess the
972 effectiveness of transmission-blocking drugs for malaria. *Future medicinal chemistry*,
973 10(22):2619–2639, 2018. 4, 5

- 974 77. Claire YT Wang, James S McCarthy, Will J Stone, Teun Bousema, Katharine A Collins,
975 and Seweryn Bialasiewicz. Assessing plasmodium falciparum transmission in mosquito-
976 feeding assays using quantitative pcr. *Malaria journal*, 17(1):249, 2018. 26
- 977 78. WHO. *World Malaria Report 2017*. World Health Organization (WHO), 2017. 27
- 978 79. WHO. Malaria vaccines. [https://www.who.int/immunization/research/
979 development/malaria/en/](https://www.who.int/immunization/research/development/malaria/en/), 2020. Last Accessed: March 30, 2021. 3
- 980 80. Wodegebriel Assefa Woldegerima. *Mathematical Modeling of the Immunopathogenesis of
981 the Within Human Host and the Within Vector Host Dynamics of the Malaria Parasite*.
982 PhD thesis, Department of Mathematics, University of Buea, Cameroon, 2018. 5
- 983 81. Woldegebriel A Woldegerima, Gideon A Ngwa, and Miranda I Teboh-Ewungkem. Sen-
984 sitivity analysis for a within-human-host immuno-pathogenesis dynamics of plasmodium
985 falciparum parasites. *Texts in Biomathematics*, 1:140–168, 2018. 17
- 986 82. Woldegebriel A Woldegerima, Miranda I Teboh-Ewungkem, and Gideon A Ngwa. The im-
987 pact of recruitment on the dynamics of an immune-suppressed within-human–host model
988 of the plasmodium falciparum parasite. *Bulletin of mathematical biology*, 81(11):4564–
989 4619, 2019. 2
- 990 83. Jianyong Wu, Radhika Dhingra, Manoj Gambhir, and Justin V Remais. Sensitivity
991 analysis of infectious disease models: methods, advances and their application. *Journal
992 of The Royal Society Interface*, 10(86):20121018, 2013. 17

993 Appendix (Mathematical analysis of the developed model)

994 Here we state and prove the basic mathematical properties of system (10). But, we start with
995 the following remarks.

996 **Remark 1** *The functions $E_a(t)$ defined in 2, $G_{IM}(t)$ and $G_{IF}(t)$ defined in 1 are nonnegative,
997 bounded and decreasing with time with the property that $0 < E_a(t) \leq \tilde{E}_{a0}$, $0 < G_{IM}(t) \leq \tilde{m}G_{I0}$,
998 $0 < G_{IF}(t) \leq (1 - \tilde{m})G_{I0} \forall t \geq 0$ with $\lim_{t \rightarrow +\infty} (E_a(t), G_{IM}(t), G_{IF}(t)) = (0, 0, 0)$.*

Remark 2 *The function $k : [0, \infty) \rightarrow [0, \infty)$ given by (8) is non-negative, bounded and con-
tinuous function of time with*

$$0 \leq k(t) \leq \kappa, \quad \forall t \geq 0, \quad \text{and} \quad \lim_{t \rightarrow (10 - \varepsilon^2)^-} k(t) = \lim_{t \rightarrow (10 - \varepsilon^2)^+} k(t) = 0 = k(0),$$

$$\lim_{t \rightarrow (10 + \varepsilon^2)^-} k(t) = \lim_{t \rightarrow (10 + \varepsilon^2)^+} k(t) = \kappa = k(10 + \varepsilon^2).$$

999 *Its plot with time is shown in Figure 2. Additionally, it is continuous modification of the*
1000 *step-function rate used in [71, 73].*

1001 Now, lets begin by defining $\mathbf{x} = (E_a, G_{IM}, G_{IF}, G_M, G_F, Z, T, O, S)^{Tr}$, (here Tr stands for
1002 transpose), to be a column vector in \mathbb{R}^9 . Then, the initial conditions of system (10) can be
1003 written as:

$$\mathbf{x}(0) = (E_a, G_{IM}, G_{IF}, G_M, G_F, Z, T, S)(0) = \left(\tilde{E}_{a0}, \tilde{m}G_{I0}, (1 - \tilde{m})G_{I0}, 0, 0, 0, 0, 0 \right), \quad (11)$$

1004 where, $\tilde{E}_{a0} \geq 0$ and $G_{l0} \geq 0$ are respectively the initial numbers per volume of ingested human
 1005 adaptive immune cells and late stage gametocytes picked by mosquito during a blood meal
 1006 from a vertebrate host. Next, lets define the biologically-feasible region $\mathcal{D}_v \subseteq \mathbb{R}_+^9$:

$$\mathcal{D}_v = \left\{ (E_a, G_{lM}, G_{lF}, G_M, G_F, Z, T, O, S) \in \mathbb{R}^9 : \begin{array}{l} E_a \geq 0, G_{lM} \geq 0, G_{lF} \geq 0, G_M \geq 0, \\ G_F \geq 0, Z \geq 0, T \geq 0, O \geq 0, S \geq 0 \end{array} \right\}.$$

Then, we can rewrite our dynamical system (10) as an initial value problem (IVP) in the form

$$\mathbf{x}' = \Phi(\mathbf{x}), \quad \mathbf{x}(0) = \mathbf{x}_0, \quad (12)$$

where, $\mathbf{x} : [0, \infty) \rightarrow \mathbb{R}^9$ is a column vector of state variables as defined, and $\Phi : \mathbb{R}^9 \times [0, \infty) \rightarrow \mathbb{R}^9$ with $\Phi(\mathbf{x}) = (\phi_1, \dots, \phi_9)^{Tr}(\mathbf{x})$ the vector valued function containing the right hand side of the system as it's components, and

$$\mathbf{x}_0 = (E_a(0), G_{lM}(0), G_{lF}(0), G_M(0), G_F(0), Z(0), T(0), O(0), S(0))^{Tr}$$

1007 be the column vector containing the initial conditions of the system. Then we have the following
 1008 theorems.

1009 **Theorem 1 (Positivity and positive invariance of solution)** *Consider system (10) with*
 1010 *initial conditions (11). If the initial data is in \mathbb{R}_+^9 , then every solution of system (10) remains*
 1011 *in \mathbb{R}_+^9 . If additionally, the initial data satisfies $\mathbf{x}(0) = \mathbf{0}$, then the solutions of system (10)*
 1012 *will remain zero for all $t > 0$. Thus, with respect to the system, \mathbb{R}_+^9 is positively invariant and*
 1013 *attracting. Additionally, the system has a forward positive solution in \mathbb{R}_+^9 , once it starts there.*

1014 **Proof of Theorem 1 (Positivity and positive invariance of solution):**

First, if $\mathbf{x}(0) = \mathbf{0} = (0, 0, 0, 0, 0, 0, 0, 0, 0)$, then using equation (12), $\mathbf{x}'(0) = \Phi(\mathbf{0}) = \mathbf{0}$. That is, each component of \mathbf{x} remains stationary at $\mathbf{0}$ if $\mathbf{x}(0) = \mathbf{0}$. If, on the other hand, any one of the components of \mathbf{x} is zero, then from system (10), it is easily seen that the differential equation corresponding to that component is non-negative and hence no trajectory of the system passes out of \mathbb{R}_+^9 through that component's zero axis. Next, to prove *positivity*, let the initial data

$$\mathbf{x}_0 = (E_a, G_{lM}, G_{lF}, G_M, G_F, Z, T, O, S)(0) \in \mathbb{R}_+^9.$$

1015 Then we want to show that every solution $(E_a, G_{lM}, G_{lF}, G_M, G_F, Z, T, O, S)(t)$ is in \mathbb{R}_+^9
 1016 for all $t \geq 0$. To begin, let

$$t^* := \sup \left\{ t > 0 \mid \begin{array}{l} E_a(t) > 0, G_{lM}(t) > 0, G_{lF}(t) > 0, G_M(t) > 0, G_F(t) > 0, Z(t) > 0, \\ T(t) > 0, O(t) > 0, S(t) > 0 \end{array} \right\}.$$

1017 If $t^* = \infty$, then all solutions of the system are positive (from the definition of t^* as a least upper
 1018 bound).

1019 Suppose $t^* < \infty$, then by the definition of t^* there is $t < t^*$ such that at least one of
 1020 $G_{lM}(t), G_{lF}(t), G_M(t), G_F(t), Z(t), T(t), O(t)$ or $S(t)$ is equal to zero at $t = t^*$. Let's check
 1021 each individually. Suppose $E_a(t^*) = 0$ with

$$\left\{ \begin{array}{l} E_a(t) > 0, G_{lM}(t) > 0, G_{lF}(t) > 0, G_M(t) > 0, G_F(t) > 0, Z(t) > 0, \\ T(t) > 0, O(t) > 0, S(t) > 0, \end{array} \right. \quad (13)$$

for $0 \leq t < t^*$. From (2), we have $E_a(t) = \tilde{E}_{a0} e^{-\tilde{\beta}t} \forall t \geq 0$, and thus $E_a(t) > 0, \forall t \geq 0$ whenever $\tilde{E}_{a0} > 0$. This is a contradiction to the assumption that there is $t^* < \infty$ such that $E_a(t^*) = 0$.

Hence, there is no such t^* . That is, $E_a(t) > 0, \forall t \geq 0$ provided that $\tilde{E}_{a0} > 0$. Next, suppose $G_{IM}(t^*) = 0$ with (13) satisfied. Then from the first equation of system (10), we have

$$G'_{IM}(t) = -c_1 G_{IM}(t), \text{ with } G_{IM}(0) = \tilde{m}G_{I0}.$$

By separating variables and integrating we get

$$G_{IF}(t) = (1 - \tilde{m})G_{I0}e^{-d_1 t}, \forall t \geq 0, \quad (14)$$

1022 and thus, $G_{IF}(t) = (1 - \tilde{m})G_{I0}e^{-d_1 t} > 0, \forall t \geq 0$, whenever $G_{IF}(0) = (1 - \tilde{m})G_{I0} > 0$. Hence,
 1023 $G_{IF}(t) > 0, \forall t \geq 0$ provided that $G_{IF}(0) > 0$. Now, let $G_M(0) > 0$ and $G_M(t^*) = 0$, with (13)
 1024 satisfied. Then from the third equation of model (10), we have

$$G'_M(t) + \left(a_1 + \frac{\beta_4 G_F(t)}{1 + \xi E_a(t)} \right) G_M(t) = s_1 \tilde{\alpha}_1 c_1 G_{IM}(t) = s_1 \tilde{\alpha}_1 c_1 \tilde{m} G_{I0} e^{-c_1 t} \quad (15)$$

which is a first order linear ODE with integrating factor (*I.F*)

$$I.F = \exp \left(\int_0^t \left(a_1 + \frac{\beta_4 G_F(\tau)}{1 + \xi E_a(\tau)} \right) d\tau \right).$$

Set

$$f_1(t) := s_1 \tilde{\alpha}_1 c_1 \tilde{m} G_{I0} e^{-c_1 t}, \quad u_1(t) = \exp \left(\int_0^t \left(a_1 + \frac{\beta_4 G_F(\tau)}{1 + \xi E_a(\tau)} \right) d\tau \right). \quad (16)$$

Clearly $f_1(t) > 0$, and $u_1(t) > 0, \forall t \geq 0$ with $u_1(0) = 1, f_1(0) = s_1 \tilde{\alpha}_1 c_1 \tilde{m} G_{I0} > 0$. Now on multiplying (15) all through by its integrating factor $u_1(t)$, we get

$$u_1(t) \frac{dG_M}{dt} \left(a_1 + \frac{\beta_4 G_F(t)}{1 + \xi E_a(t)} \right) u_1(t) G_M(t) = u_1(t) f_1(t).$$

Using product rule and then integrating from 0 to t^* yields,

$$G_M(t^*) = \frac{G_M(0)}{u_1(t^*)} + \frac{1}{u_1(t^*)} \int_0^{t^*} f_1(\tau) u_1(\tau) d\tau, \quad (17)$$

1025 where $u_1(t)$ and $f_1(t)$ as given in (16). Since $u_1(t^*) > 0$, and $f_1(t^*) > 0$, for all $t^* \geq 0$, we have
 1026 that $G_M(t^*) > 0, \forall t^* > 0$ whenever $G_M(0) > 0$. This contradicts our assumption that there is
 1027 $t^* < \infty$ defined by (13) such that $G_M(t^*) = 0$. Hence, there is no such t^* such that $G_M(t^*) = 0$.
 1028 Therefore, $G_M(t) > 0, \forall t \geq 0$ whenever the initial data is positive.

Alternatively, without solving for $G_M(t^*)$, we can show that $G_M(t^*) > 0, \forall t^* > 0$ whenever $G_M(0) > 0$. This is because the right hand side of (15), $f_1(t) := s_1 \tilde{\alpha}_1 c_1 \tilde{m} G_{I0} e^{-c_1 t}$, is always positive for all $t \geq 0$, and thus, we have

$$G'_M(t) + \left(a_1 + \frac{\beta_4 G_F(t)}{1 + \xi E_a(t)} \right) G_M(t) > 0, \forall t \geq 0.$$

On multiplying all through out by the $u_1(t)$ as defined in (16), we have

$$\frac{d}{dt} (G_M(t) u_1(t)) > 0, \forall t \geq 0. \Rightarrow G_M(t) u_1(t) \Big|_0^{t^*} > 0, \forall t \geq 0$$

1029 This implies that $G_M(t^*) > \frac{G_M(0)}{u_1(t^*)}$ and hence, $G_M(t^*) > 0, \forall t^* > 0$ whenever $G_M(0) > 0$ since
 1030 $u_1(t^*) > 0$, for all $t^* > 0$.

Next suppose $G_F(0) > 0$ and there is $t^* < \infty$ such that $G_F(t^*) = 0$ with (13) satisfied for $0 \leq t < t^*$. Then using the fourth equation of (10) and following similar steps as above, we arrive at

$$G_F(t^*) = \frac{G_F(0)}{u_2(t^*)} + \frac{1}{u_2(t^*)} \int_0^{t^*} f_2(\tau)u_2(\tau)d\tau, \quad (18)$$

1031 where

$$u_2(t^*) = \exp\left(\int_0^{t^*} \left(b_1 + \frac{\beta_4 G_M(\tau)}{1 + \xi E_a(\tau)}\right) d\tau\right) \quad \text{and} \quad f_2(t^*) = \nu_1 \tilde{\alpha}_2 d_1 (1 - \tilde{m}) G_{l0} e^{-d_1 t^*}. \quad (19)$$

1032 This implies $G_F(t^*) > 0$ since $G_F(0) > 0$, which is a contradiction to the hypothesis that there
1033 is $t^* < \infty$ such that $G_F(t^*) = 0$. Hence, $G_F(t) > 0$, for all $t \geq 0$ whenever $G_F(0) > 0$.

Using similar methods, we can show that $G_F(t)$, $Z(t)$, $T(t)$, $O(t)$ and $S(t)$ are positive for all $t \geq 0$ whenever their corresponding initial conditions are positive. Particularly, following similar steps, we get

$$Z(t^*) = \frac{Z(0)}{u_3(t^*)} + \frac{1}{u_3(t^*)} \int_0^{t^*} f_3(\tau)u_3(\tau)d\tau, \quad (20)$$

where

$$f_3(t) = \frac{\beta_4 G_M(t)G_F(t)}{1 + \xi E_a(t)}, \quad u_3(t) = \exp((\mu_z + \delta_z)t). \quad (21)$$

$$T(t^*) = \frac{T(0)}{u_4(t^*)} + \frac{\delta_z}{u_4(t^*)} \int_0^{t^*} Z(\tau)u_4(\tau)d\tau, \quad (22)$$

where $u_4(t) = \exp((\mu_T + \delta_T)t)$.

$$O(t^*) = \frac{O(0)}{u_5(t^*)} + \frac{\delta_T}{u_5(t^*)} \int_0^{t^*} T(\tau)u_5(\tau)d\tau, \quad (23)$$

where $u_5(t^*) = \exp\left(\int_0^{t^*} (\mu_O + k(\tau))d\tau\right)$.

$$S(t^*) = \frac{S(0)}{u_6(t^*)} + \frac{n\tilde{p}}{u_6(t^*)} \int_0^{t^*} k(\tau)O(\tau)u_6(\tau)d\tau, \quad (24)$$

1034 $u_6(t) = \exp(\mu_S t)$. Therefore, every forward solution of system (10) with positive initial data
1035 remains positive for $t \geq 0$. \square

1036 It guarantees that non-negative solutions are obtained only when an initial positive number
1037 of mature gametocytes or adaptive immune cells are ingested with a blood meal taken by a
1038 female feeding anopheles mosquitoes.

1039 **Theorem 2 (Boundedness of solution)** Consider system (10) with initial conditions equa-
1040 tion (11). Then every forward solution of the system in \mathbb{R}_+^9 with initial condition in \mathbb{R}_+^9 remains
1041 bounded. Furthermore, any solution of the model system (10) starting in \mathbb{R}_+^9 eventually remains
1042 in the region $\Omega_v \subset \mathbb{R}_+^9$ defined by:

$$\Omega_v := \left\{ \begin{array}{l} (E_a, G_{lM}, G_{lF}, G_M, G_F, Z, T, O, S) \in \mathbb{R}_+^9 : 0 \leq E_a \leq \tilde{E}_{a0}, \quad 0 \leq G_{lM} \leq \tilde{m}G_{l0}, \\ 0 \leq G_{lF} \leq (1 - \tilde{m})G_{l0}, \quad 0 \leq G_M \leq G_M^\infty, \quad 0 \leq G_F \leq G_F^\infty, \quad 0 \leq Z \leq Z^\infty, \\ 0 \leq T \leq T^\infty, \quad 0 \leq O \leq O^\infty, \quad 0 \leq S \leq S^\infty, \end{array} \right\} \quad (25)$$

1043 where, G_M^∞ , G_F^∞ , Z^∞ , T^∞ , O^∞ and S^∞ are the respective upper bounds of G_M , G_F , Z , T , O and
1044 S given by $G_M^\infty = \frac{s_1 \tilde{\alpha}_1 c_1 \tilde{m} G_{l0}}{a_1}$, $G_F^\infty = \frac{\nu_1 \tilde{\alpha}_2 d_1 (1 - \tilde{m}) G_{l0}}{b_1}$, $Z^\infty = \frac{\beta_4 G_M^\infty G_F^\infty}{\mu_z + \delta_z}$, $T^\infty = \frac{\delta_z Z^\infty}{\mu_T + \delta_T}$,
1045 $O^\infty = \frac{\delta_T T^\infty}{\delta_T}$ and $S^\infty = \frac{a_1 n \tilde{p} O^\infty}{\mu_s}$.

1046 **Proof of Theorem 2 (Boundedness of solution):**

Recall that $0 < E_a(t) \leq \tilde{E}_{a0}$, $\forall t \geq 0$. Thus, $E_a(t)$ is bounded for all $t \geq 0$. Next to show the boundedness of G_{LM} and G_{LF} , we have

$$G_{LM}(t) = \tilde{m}G_{l0}e^{-c_1t}, \quad G_{LF}(t) = (1 - \tilde{m})G_{l0}e^{-d_1t}.$$

It is easily seen that G_{LM} and G_{LF} are continuous decreasing functions of time t satisfying $G_{LM}(t) \rightarrow 0$ and $G_{LF}(t) \rightarrow 0$ as $t \rightarrow \infty$. Thus, $G_{LM}(t)$ and $G_{LF}(t)$ are bounded components of the solution vector of system (10) for all $t \geq 0$, satisfying

$$0 \leq G_{LM}(t) \leq \tilde{m}G_{l0}, \quad 0 \leq G_{LF}(t) \leq (1 - \tilde{m})G_{l0}, \quad \forall t \geq 0. \quad (26)$$

Now considering the equation of G'_M :

$$\begin{aligned} \frac{dG_M}{dt} &= s_1\tilde{\alpha}_1c_1G_{LM} - a_1G_M - \frac{\beta_4G_MG_F}{1 + \xi E_a} \leq s_1\tilde{\alpha}_1c_1G_{LM} - a_1G_M \\ &\leq s_1\tilde{\alpha}_1c_1\tilde{m}G_{l0} - a_1G_M, \quad \text{by (26),} \implies \frac{dG_M}{dt} + a_1G_M \leq s_1\tilde{\alpha}_1c_1\tilde{m}G_{l0}. \end{aligned}$$

Now integrating using the integration factor e^{a_1t} yields

$$G_M(t) \leq \frac{s_1\tilde{\alpha}_1c_1\tilde{m}G_{l0}}{a_1} + A_1e^{-a_1t}, \quad \forall t \geq 0,$$

1047 where A_1 is an arbitrary constant that can be determined using the initial data. Observe that
 1048 if the initial condition $G_M(0) > \frac{s_1\tilde{\alpha}_1c_1\tilde{m}G_{l0}}{a_1}$, then $A_1 > 0$ and the bound for $G_M(t)$ is decreasing
 1049 with time. If $G_M(0) = \frac{s_1\tilde{\alpha}_1c_1\tilde{m}G_{l0}}{a_1}$, then $A_1 \geq 0$ and the bound for $G_M(t)$ is non-increasing
 1050 with time. Finally, if $G_M(0) < \frac{s_1\tilde{\alpha}_1c_1\tilde{m}G_{l0}}{a_1}$, then $A_1 < 0$ and the bound for $G_M(t)$ will be an
 1051 increasing function of t . In any of the instances we see that as $t \rightarrow \infty$, $G_M(t) \leq \frac{s_1\tilde{\alpha}_1c_1\tilde{m}G_{l0}}{a_1}$. So,
 1052 we have

$$\limsup_{t \rightarrow \infty} G_M(t) \leq \frac{s_1\tilde{\alpha}_1c_1\tilde{m}G_{l0}}{a_1}.$$

Thus, by definition of \limsup there exists $\epsilon_1 > 0$, such that

$$0 \leq G_M(t) \leq \frac{s_1\tilde{\alpha}_1c_1\tilde{m}G_{l0}}{a_1} + \epsilon_1, \quad \forall t \geq 0. \quad (27)$$

So there exist $0 \leq G_M^\infty = \frac{s_1\tilde{\alpha}_1c_1\tilde{m}G_{l0}}{a_1} < \infty$ such that

$$0 \leq G_M(t) \leq G_M^\infty, \quad \forall t \geq 0. \quad (28)$$

1053 Hence, $G_M(t)$ is a bounded component of the solution vector of system (10), for all $t \geq 0$.

1054 Similarly, we can show that $\lim_{t \rightarrow \infty} \sup G_F(t) \leq \frac{\nu_1\tilde{\alpha}_2d_1(1-\tilde{m})G_{l0}}{b_1}$, $\lim_{t \rightarrow \infty} \sup Z(t) \leq \frac{\beta_4G_M^\infty G_F^\infty}{\mu_z + \delta_z}$,
 1055 $\lim_{t \rightarrow \infty} \sup T(t) \leq \frac{\delta_z Z^\infty}{\mu_T + \delta_T}$, $\lim_{t \rightarrow \infty} \sup O(t) \leq \frac{\delta_T T^\infty}{\delta_T}$ and $\lim_{t \rightarrow \infty} \sup S(t) \leq \frac{\tilde{a}n\tilde{p}O^\infty}{\mu_s}$, where we
 1056 used $k(t) \leq \tilde{a} < \infty$, for all $t \geq 0$ since $k(t)$ given in (8) is a bounded non-negative function of t .

1057 Therefore, each forward solution is bounded with upper bounds $E_a^\infty = \tilde{E}_{a0}$, $G_{LM}^\infty = \tilde{m}G_{l0}$,
 1058 $G_{LF}^\infty = (1 - \tilde{m})G_{l0}$, $G_M^\infty = \frac{s_1\tilde{\alpha}_1c_1\tilde{m}G_{l0}}{a_1}$, $G_F^\infty = \frac{\nu_1\tilde{\alpha}_2d_1(1-\tilde{m})G_{l0}}{b_1}$, $Z^\infty = \frac{\beta_4G_M^\infty G_F^\infty}{\mu_z + \delta_z}$, $T^\infty =$
 1059 $\frac{\delta_z Z^\infty}{\mu_T + \delta_T}$, $O^\infty = \frac{\delta_T T^\infty}{\delta_T}$ and $S^\infty = \frac{\tilde{a}n\tilde{p}O^\infty}{\mu_s}$. Moreover, the set Ω_v defined in (25) is positively
 1060 invariant.

1061 \square

1062 **Theorem 3 (Uniqueness of solution)** Model (10) which is written as an initial value prob-
 1063 lem in eqn. (12) has a unique non-negative solution which remains bounded.

1064 **Proof of Theorem 3 (Uniqueness of solution):**

1065 We use the Picard-Cauchy-Lipschitz theorem for existence and uniqueness of solution, see
 1066 [36]. Thus, we are required to show that the right hand side function Φ is \mathcal{C}^1 and Lipschitz
 1067 in $U \times [0, T]$ where $U \subset \mathbb{R}_+^9$ is an open set and $[0, T] \subset [0, \infty)$. But it is known from theory
 1068 of ordinary differential equations that to show that Φ is Lipschitz continuous, it suffices to
 1069 show that the partial derivative $\frac{\partial \Phi}{\partial x_i}$ exists, continuous and bounded, $\forall i = 0, 1, 2, \dots, 8$ where
 1070 $(x_0, x_1, x_2, x_3, x_4, x_5, x_6, x_7, x_8) = (E_a, G_{IM}, G_{IF}, G_M, G_F, Z, T, O, S)$.

1071 We recall that every differentiable function is continuous. From the first equation of (10),
 1072 we observe that $\phi_0(\mathbf{x}) = -\tilde{\beta}E_a$ is continuous since it is a constant multiple of a differentiable
 1073 function E_a . Similarly, $\phi_1(\mathbf{x}) = -c_1G_{IM}$ is continuous, so does G_{IF} . From the third equation of
 1074 (10), $\phi_3 = s_1\tilde{\alpha}_1c_1G_{IM} - a_1G_M - \frac{\beta_4G_MG_F}{1+\xi E_a}$, is a linear combination of a constant (continuous) and
 1075 differentiable functions $G_{IM}(t)$, $G_M(t)$, G_M , $G_F(t)$ and $E_a(t)$. Hence, ϕ_3 is continuous since
 1076 any linear combination of continuous terms is also continuous.

1077 Similarly, $\phi_4(\mathbf{x}), \dots, \phi_8(\mathbf{x})$ are linear combination of differentiable functions (continuous)
 1078 and therefore they are all continuous. We next show that for each $i = 0, 1, \dots, 8$, $\frac{\partial \Phi}{\partial x_i}$ is
 1079 continuous and bounded. But $\frac{\partial \Phi}{\partial x_i}$ is continuous if each $\frac{\partial \phi_j}{\partial x_i}$ is continuous $\forall i, j = 0, 1, \dots, 8$. We
 1080 next show that each function $\phi_j, j = 0, 1, \dots, 8$ in the right had side of (10) is \mathcal{C}^1 , that is, $\frac{\partial \phi_j}{\partial x_i}$
 1081 is continuous.

1082 It is to show that $\frac{\partial \phi_j}{\partial x_i}$ exists and are continuous and hence $\Phi \in \mathcal{C}^1$ since each partial
 1083 derivatives consist of constants and continuous functions

1084 Next we show that $\frac{\partial \Phi}{\partial \mathbf{x}}$ is bounded, that is, $\|\frac{\partial \Phi}{\partial \mathbf{x}}\|_\infty$ is bounded for $\mathbf{x} = (E_a, G_{IM}, G_{IF}, G_M, G_F, Z, T, O, S)$,

1085 where $\frac{\partial \Phi}{\partial \mathbf{x}} = \frac{\partial}{\partial x_i} \begin{pmatrix} \phi_0, \\ \phi_1 \\ \vdots \\ \phi_8 \end{pmatrix}, \quad i = 0, 1, 2, \dots, 8.$

Using maximum norm, we have

$$\left\| \frac{\partial \Phi}{\partial E_a} \right\|_\infty = \max \left\{ |-\tilde{\beta}|, |0|, |0|, \left| -\frac{\beta_4 \xi G_M G_F}{(1 + \xi E_a)^2} \right|, \left| -\frac{\beta_4 \xi G_M G_F}{(1 + \xi E_a)^2} \right|, \left| \frac{\beta_4 \xi G_M G_F}{(1 + \xi E_a)^2} \right|, |0|, |0|, |0| \right\} < \infty,$$

1086 since we have already proved that $G_M(t)$ and $G_F(t)$ are bounded for all $t \geq 0$.

Continuing to the next component, we have

$$\frac{\partial \Phi}{\partial G_{IM}} = \frac{\partial}{\partial G_{IM}} \begin{pmatrix} \phi_1 \\ \vdots \\ \phi_8 \end{pmatrix} = (0, -c_1, 0, 0, 0, 0, 0, 0, 0)^{Tr}$$

Using the maximum norm, we get

$$\left\| \frac{\partial \Phi}{\partial G_{IM}} \right\|_\infty = \max \left\{ |0|, |-c_1|, |0|, |0|, |0|, |0|, |0|, |0|, |0| \right\} = c_1 < \infty.$$

Similarly,

$$\left\| \frac{\partial \Phi}{\partial G_{IF}} \right\|_\infty = \max \left\{ |0|, |-d_1|, |0|, |0|, |0|, |0|, |0|, |0| \right\} = d_1 < \infty,$$

$$\left\| \frac{\partial \Phi}{\partial G_M} \right\|_\infty = \max \left\{ |0|, |0|, \left| -a_1 - \frac{\beta_4 G_F}{1 + \xi E_a} \right|, \left| -\frac{\beta_4 G_F}{1 + \xi E_a} \right|, \left| \frac{\beta_4 G_F}{1 + \xi E_a} \right|, |0|, |\delta_T|, |0| \right\} < \infty.$$

1087 Similarly, we can compute the remaining norms and we obtain $\left\| \frac{\partial \Phi}{\partial x_i} \right\|_{\infty}$ for each $x_i \in \{G_F, Z, T, O, S\}$.
1088 Therefore, we conclude that $\frac{\partial \Phi}{\partial \mathbf{x}}$ is bounded for all variables $\mathbf{x} = (E_a, G_{IM}, G_{IF}, G_M, G_F, Z, T, O, S)$.
1089 Since $\frac{\partial \Phi}{\partial \mathbf{x}}$ exists, is continuous and bounded, Φ is Lipschitz continuous, then by the existence
1090 and uniqueness theorem, model (10) has a unique solution. \square

1091 While proving the positivity of solution in Theorem 1, we also have showed the lemma. The
1092 general solution to system (10) is given below in the next lemma.

1093 **Lemma 1 (General Solution of System (10))** *The unique non-negative bounded solution,*
1094 $(E_a(t), G_{IM}(t), G_{IF}(t), G_M(t), G_F(t), Z(t), T(t), O(t), S(t))^{Tr} \in \mathbb{R}_+^9$, *of system (10) with ini-*
1095 *tial condition in (11) at any $t \geq 0$ is given as:*

$$\left\{ \begin{array}{l} E_a(t) = \tilde{E}_{a0} e^{-\tilde{\beta}t}, \quad G_{IM}(t) = \tilde{m} G_{I0} e^{-c_1 t}, \quad G_{IF}(t) = (1 - \tilde{m}) G_{I0} e^{-d_1 t}, \\ G_M(t) = \frac{1}{u_1(t)} \int_0^t f_1(\tau) u_1(\tau) d\tau, \quad G_F(t) = \frac{1}{u_2(t)} \int_0^t f_2(\tau) u_2(\tau) d\tau, \\ Z(t) = \frac{1}{u_3(t)} \int_0^t f_3(\tau) u_3(\tau) d\tau, \quad T(t) = \frac{\delta_z}{u_4(t)} \int_0^t Z(\tau) u_4(\tau) d\tau, \\ O(t) = \frac{\delta_T}{u_5(t)} \int_0^t T(\tau) u_5(\tau) d\tau, \quad S(t^*) = \frac{n\tilde{p}}{u_6(t^*)} \int_0^{t^*} k(\tau) O(\tau) u_6(\tau) d\tau, \end{array} \right. \quad (29)$$

1096 where,

$$f_1(t) := s_1 \tilde{\alpha}_1 c_1 \tilde{m} G_{I0} e^{-c_1 t}, \quad f_2(t) = \nu_1 \tilde{\alpha}_2 d_1 (1 - \tilde{m}) G_{I0} e^{-d_1 t}, \quad f_3(t) = \frac{\beta_4 G_M(t) G_F(t)}{1 + \xi E_a(t)},$$

1097 and

$$\left. \begin{array}{l} u_1(t) = \exp \left(\int_0^t \left(a_1 + \frac{\beta_4 G_F(\tau)}{1 + \xi E_a(\tau)} \right) d\tau \right), \quad u_2(t^*) = \exp \left(\int_0^{t^*} \left(b_1 + \frac{\beta_4 G_M(\tau)}{1 + \xi E_a(\tau)} \right) d\tau \right), \\ u_3(t) = \exp((\mu_z + \delta_z)t), \quad u_4(t) = \exp((\mu_T + \delta_T)t), \\ u_5(t) = \exp \left(\int_0^t (\mu_O + k(\tau)) d\tau \right), \quad u_6(t) = \exp(\mu_S t) \end{array} \right\}.$$